
**Liquid Crystals**
Publication details, including instructions for authors and subscription information:
http://www.informaworld.com/smpp/title~content=t713926090

# Banana-calamitic dimers: unexpected mesophase behaviour by variation of the direction of ester linking groups in the bent-core unit

Maria Gabriela Tamba[a]; Ute Baumeister[a]; Gerhard Pelzl[a]; Wolfgang Weissflog[a]
[a] Institut für Physikalische Chemie, Martin-Luther-Universität Halle-Wittenberg, Halle, Germany

Online publication date: 06 July 2010

**To cite this Article** Tamba, Maria Gabriela , Baumeister, Ute , Pelzl, Gerhard and Weissflog, Wolfgang(2010) 'Banana-calamitic dimers: unexpected mesophase behaviour by variation of the direction of ester linking groups in the bent-core unit', Liquid Crystals, 37: 6, 853 — 874
**To link to this Article: DOI:** 10.1080/02678291003798172
**URL:** http://dx.doi.org/10.1080/02678291003798172

*Liquid Crystals,*
Vol. 37, Nos. 6–7, June–July 2010, 853–874

Taylor & Francis
Taylor & Francis Group

## INVITED ARTICLE

# Banana-calamitic dimers: unexpected mesophase behaviour by variation of the direction of ester linking groups in the bent-core unit

Maria Gabriela Tamba, Ute Baumeister, Gerhard Pelzl and Wolfgang Weissflog*

*Institut für Physikalische Chemie, Martin-Luther-Universität Halle-Wittenberg, von-Danckelmann-Platz 4, 06120 Halle, Germany*

(*Received 19 November 2009; accepted 11 March 2010*)

A five-ring bent-core unit and a phenyl benzoate moiety are linked together by means of a flexible spacer. Starting from dimers having different length of the aliphatic parts, that is the terminal alkyloxy chains and the spacer, the direction of each of the four ester connecting groups in the bent-core unit is reversed step by step. In this way thermodynamically stable polar and non-polar mesophases in unusual sequences could be obtained. For instance, a $SmC_sP_{AF}$–$SmC'_sP_{AF}$ transition and the existence of two nematic phases (N, $N_X$) have been observed. The nematic phases of the banana-calamitic dimers exhibit unusual properties comparable to those of the nematic phases reported for some monomeric bent-core mesogens. The electric field-induced enhancement of the SmCP–SmA transition temperature of one compound proves the existence of polar clusters already in the non-polar SmA phase.

**Keywords:** liquid crystalline dimers; bent-core mesogens; nematic–nematic transition; ferroelectric behaviour



## 1. Introduction

Liquid crystalline dimers are a subject both of traditional and of topical interest. Vorländer had already reported in the 1920s on twin molecules, their liquid crystalline properties and the distinct alternation of the clearing temperatures dependent on the number of carbon atoms in the spacer [1]. Several excellent reviews show the actuality of dimers and oligomers in material science [2–6]. Liquid crystalline dimers are of interest because the coupling of two simple mesogens (in this context called monomers) by means of a flexible aliphatic spacer results in medium-mass compounds which can exhibit qualitatively new properties. This is important with respect to high-molecular compounds because a further linear increase of the molecules to trimers, tetramers, and higher oligomers finally gives polymers.

The dimers themselves are also a subject of extensive research. Dimers have a modular design and each module can be systematically varied. Liquid crystalline dimers can have a symmetric or non-symmetric structure, and all types of mesogens such as calamitic, discotic, phasmidic, or bent-core ones can be linked together. The position of the connection can be different, too. For example, two calamitic mesogenic units can be linked to each other in terminal–terminal, terminal–lateral and lateral–lateral positions. As expected, the properties of all these compounds differ greatly, because the shape of the dimers depends on these connecting points: they may be linear, T-shaped or H-shaped. [3, 7–10]. Furthermore, the properties of simple terminal–terminal-linked calamitic dimers strongly depend on the length and parity of all the aliphatic parts, that is, the length of the terminally attached hydrocarbon chains and the length of the aliphatic spacer. This is caused by frustration effects which influence the packing of the molecules in the mesophases [3]. To give a representative example, the inverse phase sequence SmC–SmA with decreasing temperature was reported for calamitic dimers. This depends on the ratio of the aliphatic parts, that is on the length of both the spacer and on the terminally attached hydrocarbon chains [11]. As has been long known, the shape of linear twin molecules alternates with the number of single units in the flexible aliphatic spacer: even-numbered spacers give more or less linear molecules, but odd-numbered spacers result in more bent-shaped molecules.

Considering this, in 1995 we started the search for materials which might be able to form polar layer structures. The spacer was selected to be odd-numbered and, in addition, perfluoro substituted to use the effect of microsegregation [12]. Alfred Saupe was highly interested in this concept which was, however, overtaken by the banana concept in 1996 [13]. In the meantime Takezoe *et al.* [14, 15] have proved that simple odd-numbered calamitic dimers are able to form a polar smectic phase if a special ratio between the length of the terminal aliphatic chains and the spacer is fixed, that means a short spacer and long terminal hydrocarbon groups. Bialecka-Florjanczyk *et al.* [16] reported an odd–even effect in a series of

*Corresponding author. Email: wolfgang.weissflog@chemie.uni-halle.de

ISSN 0267-8292 print/ISSN 1366-5855 online

DOI: 10.1080/02678291003798172
http://www.informaworld.com

dimers: only the homologues having an odd-numbered spacer are able to form the banana phase $B_4$. For a dimer with a relatively long even-numbered spacer, a slightly bent molecular shape has been predicted in a smectic phase to explain properties which are strongly reminiscent of $B_7$ phases formed by banana-shaped molecules [17]. The use of molecular fragments able to show microsegregation supports frustration effects and can result in materials with new phase sequences. There are several reports of dimers with oligo(siloxane), oligo(ethyleneglycol) and perfluoroalkyl fragments in the spacer [2–6]. On the other hand, a $SmA_L$–$SmA_H$ transition was observed for linear twin molecules bearing perfluoroalkyl chains in both terminal positions [18].

Some examples of dimers containing bent-core mesogenic units have been reported in the literature. Bent-core mesogens, also named as banana-shaped liquid crystals, have been a subject of topical interest in the field of liquid crystals since 1996 [19–21]. Due to their shape they are able to exhibit polar order in smectic layers, which can be switched by applying an electric field. Previously, such ferro- and antiferroelectric behaviour has been observed for chiral compounds only. Furthermore, a tilt of the molecular long axis with respect to the layer normal can result in supramolecular layer chirality, although the molecules are non-chiral themselves. Using polarising microscopy this chirality can be directly observed by the existence of chiral domains of different handedness and by the nucleation of helical germs on cooling the isotropic liquid, especially in the case of $B_7$ phases.

If two bent-core monomers are terminally connected together, a strong influence of the chemical structure and the parity of the spacer was observed. In 2002 Tschierske *et al.* prepared the first dimers of this type [22]. The SmCP phases observed for these compounds exhibit ferro- and antiferroelectric behaviour, dependent on the number of dimethylsiloxane units [22, 23]. Such a relationship also exists for carbosilane-connected twin molecules [24, 25]. In contrast, if alkylene spacers and oligo(oxyethylene) spacers are used, the formation of SmC or columnar phases is preferred [23, 26]. Applying an electric field, these columnar phases do not show any current response which means these are not polar phases. Attachment of lateral fluoro atoms to the aromatic rings of comparable compounds results in the formation of polar columnar phases, as reported by Umadevi *et al.* [27, 28].

The synthesis of dimers consisting of a bent-core and a calamitic mesogenic unit needs much more synthetic work. This could be one reason why research on such non-symmetric twin molecules is still in its infancy. Very few compounds have been reported up to now, although these materials can exhibit very interesting properties. Yelamaggad *et al.* have reported latently biaxial nematic phases for a compound consisting of a five-ring bent-core mesogenic moiety and cyanobiphenyl [29, 30]. The nematic phase of a corresponding trimer built from two cyanobiphenyl units connected to a five-ring bent-core monomer, however, gives no hint for biaxial behaviour. The same research group have prepared dimers, in which a cholesteryl unit is connected with a banana-shaped monomer. Some of these compounds are characterised by a broad existence range of a blue phase [29, 31, 32].

In 2006 we reported three banana-calamitic dimers consisting of a five-ring bent-core unit which is coupled by an aliphatic spacer to alkyloxy substituted calamitic monomers [33]. Only the compound containing a three-ring calamitic part exhibits an enantiotropic nematic and a columnar phase. If two-ring calamitic moieties are used, the mesophases are metastable only. There are strong hints that nematic phases formed by this type of dimer exhibit very interesting properties. For example, the formation of unusual electroconvection patterns was reported by Heuer *et al.* [34, 35], but also a field-induced texture transition and the occurrence of a metastable biaxial nematic state is of current interest [36].

Up to now there have been no systematic studies on banana-calamitic dimers. The task of the present work was to investigate the chemical structure–properties relationships for this relatively new type of twin-molecule. We aimed to prepare compounds which exhibit different enantiotropic mesophases, and which might represent suitable materials for further physical investigations. These dimers represent compounds at the boundary between banana-shaped and calamitic liquid crystals, a good precondition to design materials which have extraordinary properties.

## 2. Experiment

### *2.1 Physical methods*

The phase transition temperatures and transition enthalpies were determined using a differential scanning calorimeter DSC Pyris 1 (Perkin Elmer). The optical textures and field-induced texture changes were examined using a polarising microscope DMRXP (Leica) equipped with a hot stage HT80 and an automatic temperature controller (Mettler Toledo). The switching polarisation was measured by employing the triangular-wave voltage method [37]. The liquid crystalline material was loaded into commercial electro-optical cells (EHC Corp. Tokyo). X-ray diffraction measurements on powder-like samples were performed using a Guinier film camera (Huber Diffraktiontechnik GmbH). X-ray

investigations on aligned samples were carried out with an area detector (HI-STAR, Siemens/Bruker). Alignment was obtained by long annealing of a drop of the liquid crystal on a glass plate after slow cooling of the isotropic liquid, or by applying a magnetic field of about 1 T to a nematic sample in a glass capillary in a temperature-controlled heating stage.

### 2.2 *Synthesis of the banana-calamitic dimers*

The compounds under study consist of a five-ring bent-core moiety and a two-ring calamitic unit. Both mesogenic parts are connected by an aliphatic spacer. All aliphatic parts that are both terminal chains and the hydrocarbon spacer are linked to the aromatic rings by ether groups. Furthermore, all phenyl rings are connected to each other by carboxylic groups. To synthesise these compounds reactions have been used, well-known in organic chemistry: Williamson etherification reaction, Mitsunobu reaction, esterification of phenolic parts with fragments containing benzoic acids by means of dicyclohexylcarbodiimide or the acid chloride method. The strategically crucial point is to find the best linking position in the final reaction step which allows an effective purification, because the solubility and chromatographic properties of the intermediates and final products are not so different. We decided to design a four-ring bent-core moiety **B** and a calamitic part **C** containing one phenyl ring, which are connected to each other by the flexible spacer group. The final step is sketched as retro-synthesis in Scheme 1.

(a)

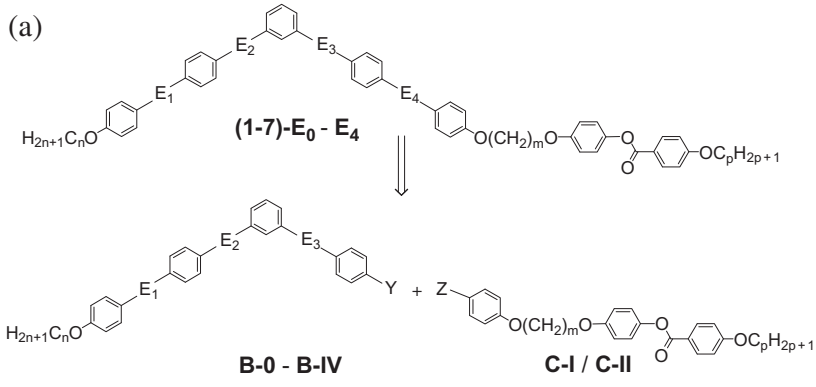


***Y*** = COOH; OH; ***Z*** = OH;COOH;

(b)

| Comp. No. | $E_1$ | $E_2$ | $E_3$ | $E_4$ |
|---|---|---|---|---|
| **(1–7)-$E_0$** | COO | COO | OOC | OOC |
| **(1–7)-$E_1$** | **OOC** | COO | OOC | OOC |
| **(1–7)-$E_2$** | COO | **OOC** | OOC | OOC |
| **(1–7)-$E_3$** | COO | COO | **COO** | OOC |
| **(1–7)-$E_4$** | COO | COO | OOC | **COO** |

(c)

| Comp. No. | *n* | *m* | *p* |
|---|---|---|---|
| **1** | 12 | 3 | 6 |
| **2** | 8 | 6 | 6 |
| **3** | 12 | 6 | 6 |
| **4** | 16 | 6 | 6 |
| **5** | 12 | 6 | 12 |
| **6** | 12 | 11 | 6 |
| **7** | 12 | 11 | 12 |

Scheme 1. (a) Final reaction step used to prepare the banana-calamitic dimers; general formula using the retro-synthetic presentation; (b) table of the final compounds comprising the corresponding orientation of the ester linking groups; COO groups having an inverse direction in comparison to those of the reference compounds (1–7)-$E_0$ are marked in red (colour online); (c) table of the final compounds listing the corresponding length of the terminal chain at the bent-core unit (*n*), the spacer length (*m*) and the length of the terminal chain at the calamitic moiety (*p*).

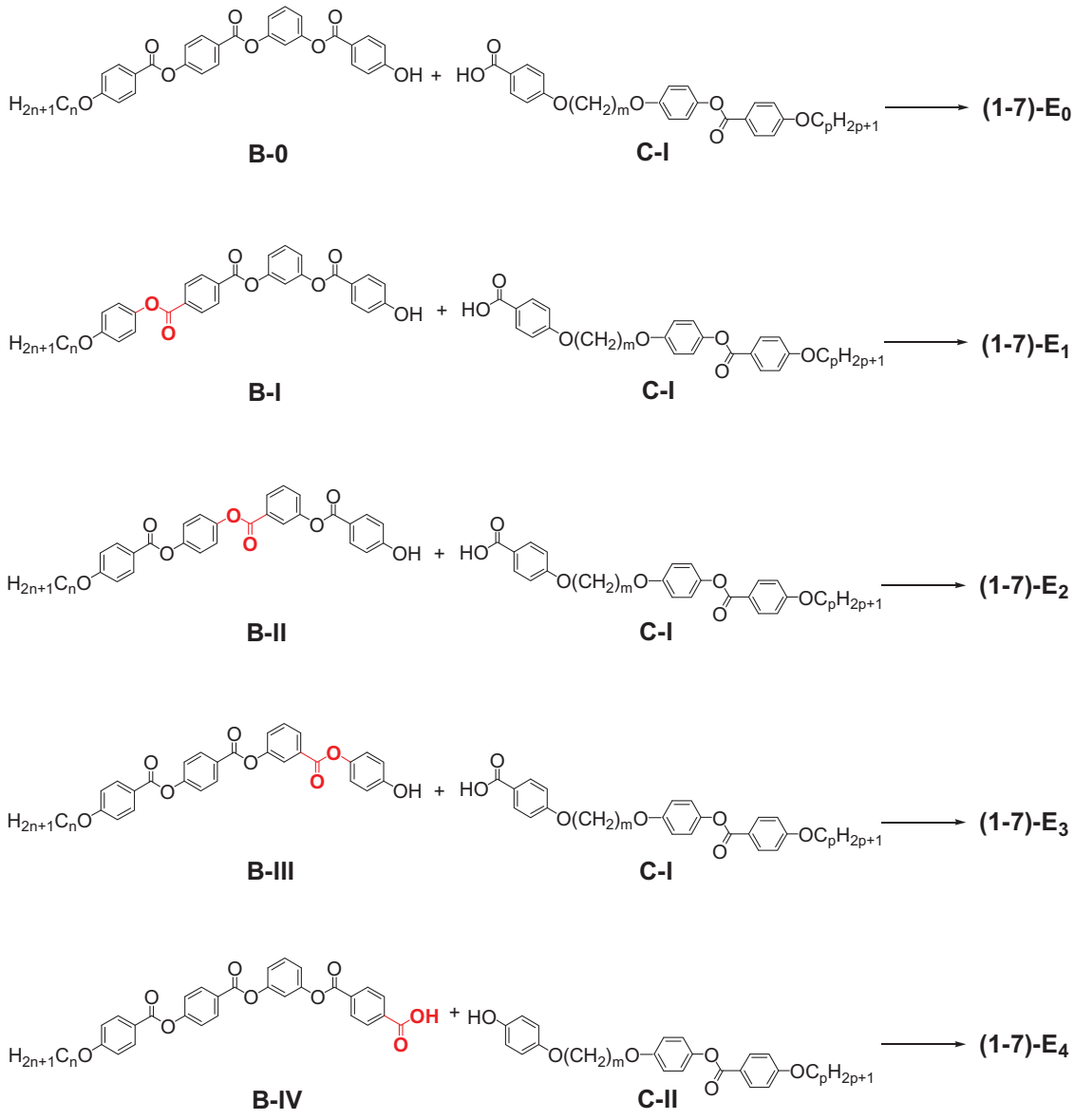


Scheme 2. Final reaction steps used to prepare the banana-calamitic dimers. The final products $\mathbf{E_0}$ to $\mathbf{E_4}$ were obtained by esterification of the bent four-ring moieties **B-0** to **B-IV** with the calamitic units **C-I** to **C-II**.

The preparation of the reference compounds $\mathbf{E_0}$ has been reported previously by us and is shown only for comparison [33]. The compound $\mathbf{E_1}$ results from the esterification of the four-ring phenol **B-I** with the acid **C-I**; both intermediates have also been described by us previously [26, 33]. To demonstrate the reaction pathway in more detail, the synthesis of the compounds **3-E$_2$** and **3-E$_4$** is shown in Scheme 3 and 4.

The compound **3-E$_2$** was selected to illustrate the synthesis of a bent four-ring moiety (see Scheme 3). Intermediates containing two functional groups have been mono-protected, in most cases by the benzyl group, which can be simply deprotected by hydrogenation. This approach is not possible for the preparation of the 3-[4-benzyloxy(benzoyloxy)benzoic acid], therefore the oxidation of the corresponding 3-formylphenyl 4-benzyloxybenzoate was performed (see step (ii) in Scheme 3). After deprotection the benzyl group, the esterification of the four-ring phenol **B-II** with the calamitic moiety **C-I**, which brings the fifth phenyl ring for the bent-core mesogenic unit, results in the final product **3-E$_2$**. Isolation and purification of the end product was achieved by repeated chromatography and crystallisation. Compound **3-E$_2$** was purified by column chromatography on silica (eluent chloroform/ethyl acetate

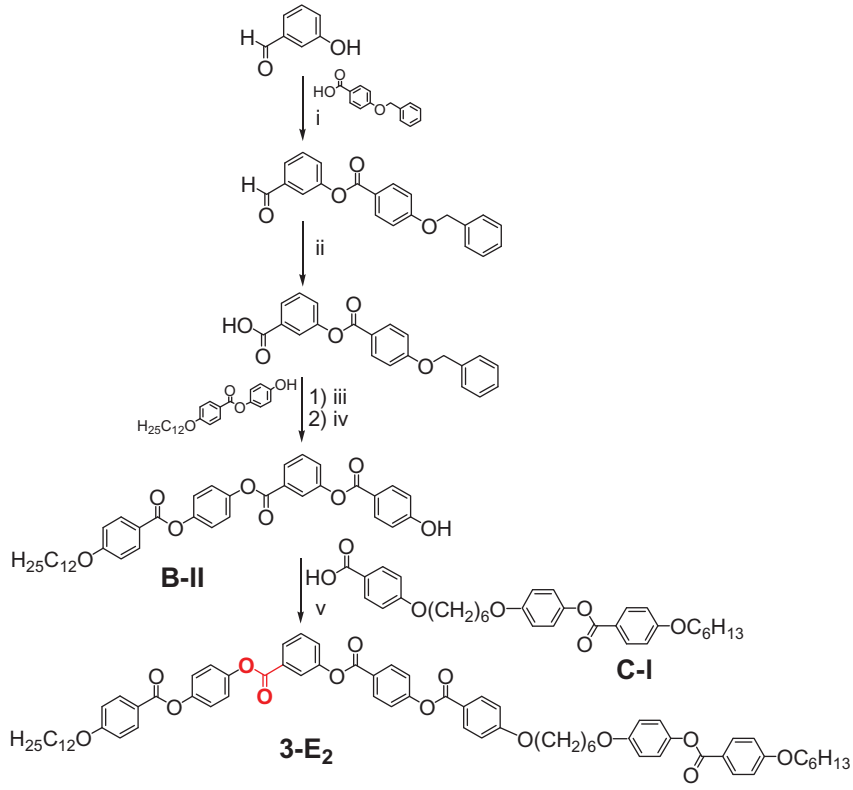


Scheme 3. Synthesis of compound **3-E$_2$**: (i),(iii),(v) DCC, DMAP, $CH_2Cl_2$, 6 h, RT; (ii) resorcinol, $NaClO_2$, $NaH_2PO_4$, THF/$H_2O$, 24 h, RT; (iv) $H_2$, Pd/C, ethyl acetate, 24 h, RT.



10:0.1) followed by crystallisation from ethyl acetate/ethanol.

The reaction pathway to prepare compound **3-E$_4$** is shown in Scheme 4. The attachment of the aliphatic spacer group to the calamitic moiety is a key reaction, therefore three different reaction types were investigated. Step (i) is an etherification using NaH to form the corresponding sodium phenolate, which can react with 6-chlorohexanol. Due to the modest reactivity of the chloro compound the yields were relatively low. The etherification of 4-hydroxyphenyl 4-n-hexyloxybenzoate with 1,6-dibromohexane (step (ii)) is done under well-known conditions. Long reaction times are necessary in butan-2-one as solvent. However, the purity of the resulting intermediate is higher than that which the reaction in dimethylformamide gives at higher temperatures. The same intermediate has been obtained by the Mitsunobu reaction in high yields and good quality, see step (iii) in Scheme 4. Here, the high cost of the 6-bromohexanol is a disadvantage. After the etherification with 4-benzyloxyphenol (steps (iv), (v)) deprotection (step (vi)), the esterification of the phenol **C-II** with the four-ring benzoic acid **B-IV** [26] results in compound **3-E$_4$**, which was purified as described for compound **3-E$_2$**.

## 3. Results

The main subject of this paper is a systematic study on the influence of the direction of the ester linking groups on the mesophase behaviour of banana-calamitic dimers. To obtain comparable results, the following molecular parameters have been selected: the bent-core unit contains five phenyl rings which are all connected by carboxylic groups E; the calamitic unit is a phenyl benzoate; alkyloxy chains are attached to the two terminal positions; and the alkylene spacer is linked to both mesogenic moieties by ether oxygens.

Variations were made in the length *n* and *p* of the terminal hydrocarbon chains and in the number *m* of methylene units in the aliphatic spacer. After that, the direction of each of the four ester groups between the phenyl rings of the bent-core unit was inverted. The *reference compounds* $E_0$ have a bent-core unit possessing a central resorcinol fragment and both ester linking groups within one leg have the same direction. Since for each group of isomers the direction of only one ester group has been changed, the inversion of the first, second, third and fourth results in compounds which are assigned as **E$_1$**, **E$_2$**, **E$_3$** and **E$_4$**, respectively (general formula, see Scheme 5).

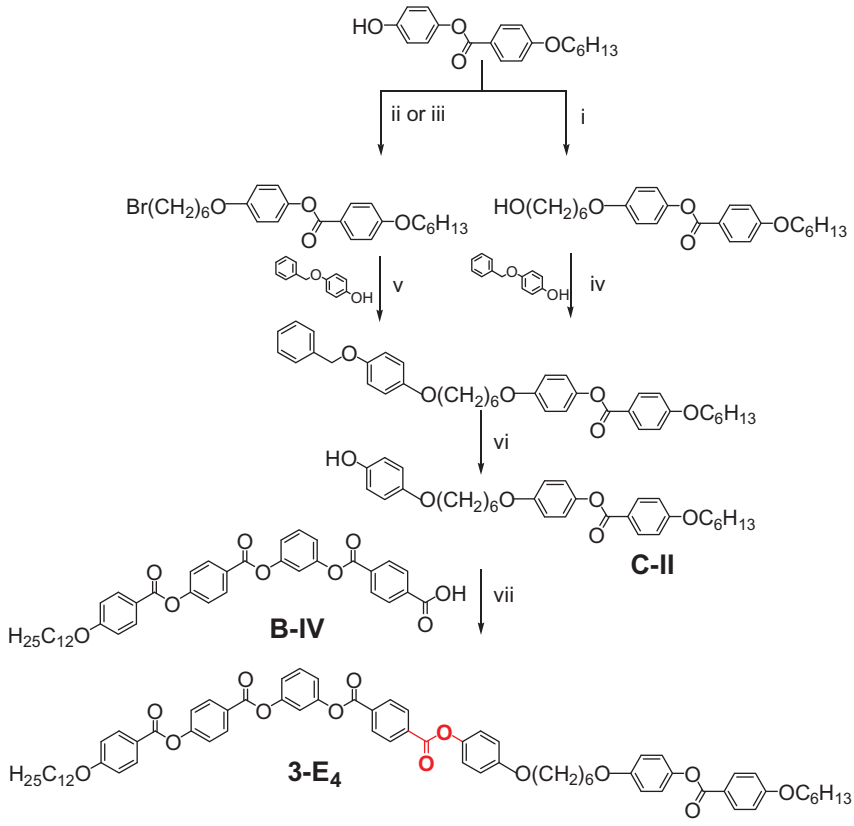


Scheme 4. Synthesis of compound **3-E$_4$**: (i) $Cl(CH_2)_6OH$, NaH, DMF, 48 h, RT; (ii) $Br(CH_2)_6Br$, $K_2CO_3$, $Bu_4NI$, butan-2-one, reflux 48 h; (iii) $HO(CH_2)_6Br$, $Ph_3P$, DEAD, THF, 1 h, 0°C, 48 h, RT; (iv) $Ph_3P$, DEAD, THF, 1 h, 0°C, 48 h, RT; (v) $K_2CO_3$, $Bu_4NI$, DMF, 24 h, 80°C; (vi) $H_2$, Pd/C, ethyl acetate, 24 h, RT; (vii) DCC, DMAP,$CH_2Cl_2$, 6 h, RT.

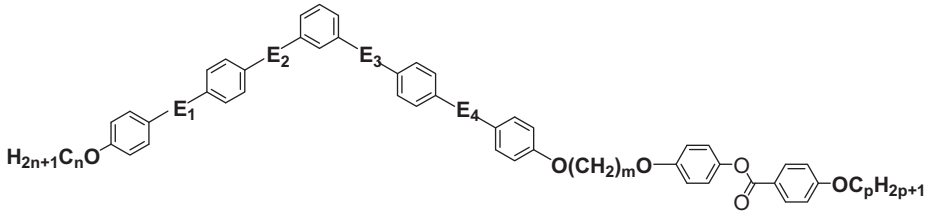


Scheme 5. General formula of the banana-calamitic dimers under study.

To explain the system of abbreviations, an example is given in Scheme 6. The reference compound **2-E$_0$** is derived from resorcinol, and the aliphatic chains have the lengths $n = 8$; $m = 6$; $p = 6$. For compound **2-E$_3$** the aliphatic chains are the same; however, the direction of the carboxylic group in position $E_3$ is inversed.

The mesophase behaviour of the reference compounds **1-E$_0$** to **7-E$_0$** is given in Table 1 for comparison only. Extensive physical measurements, such as polarising microscopy, X-ray and electro-optical studies of these reference compounds will be described elsewhere [38]. The mesophase behaviour of the compounds **E1**–**E4**, the transition temperatures and the associated transition enthalpies, lattice parameters and $P_S$ values of the prepared banana-calamitic dimers are given in Table 1. The compounds are listed and will be discussed with respect to increasing length of the spacer group and increasing length of the terminal alkyloxy chains. To provide more information, the mesophase behaviour on cooling is sketched in the bar charts, the transition temperatures are taken from the first differential scanning calorimetry (DSC) cooling scan (10 K min$^{-1}$), therefore the recrystallisation temperatures can also be presented.

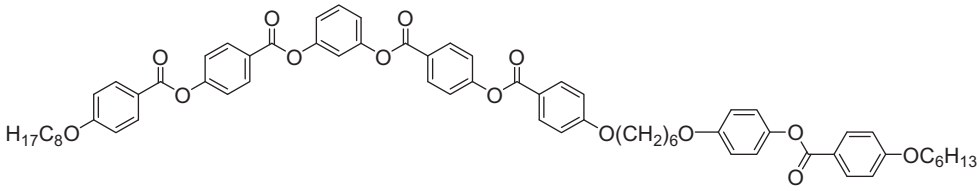


2- **E$_0$** ($n=8$; $m=6$; $p=6$) Cr 145 (M1 125 SmC$_s$P$_{FE}$ 130) N 151 I

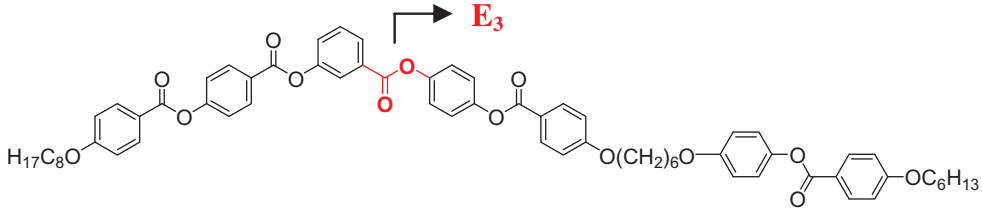


2-**E$_3$** ($n=8$; $m=6$; $p=6$) Cr 147 (Col$_x$ 127 N$_x$ 129) N 167 I

Scheme 6. Example explaining the abbreviation system for the banana-calamitic dimers.



### *3.1 Compounds 1-E$_0$ and 1-E$_2$ ($n = 12$; $m = 3$; $p = 6$)*

Compounds **1** have the shortest spacers with $m = 3$. The reference dimer **1-E$_0$** exhibits a monotropic Col$_r$P$_{AF}$ phase. The inversion of the second ester linking group E$_2$ in the bent-core mesogenic unit results in a loss of the liquid crystalline properties for the dimer **1-E$_2$**. No significant differences could be observed in the melting temperature of the two isomers (see Table 1); however, the recrystallisation temperatures are different, see Figure 1. Further synthetic variation seems to be not helpful in series **1**.

### *3.2 Compounds 2-E$_0$, 2-E$_2$ and 2-E$_3$ ($n = 8$; $m = 6$; $p = 6$)*

In the compounds **2** the number $m$ of methylene groups in the spacer is 6, and both terminal alkyloxy chains have a comparable length ($n = 8$; $p = 6$), see Figure 2. The dimer **2-E$_0$** with all ester linking groups in the reference orientation (**E$_0$**) exhibits one enantiotropic nematic phase and two monotropic phases (SmC$_s$P$_{FE}$ and an unclassified mesophase designated as the M$_1$ phase).

The isomeric dimer **2-E$_2$** with the carboxylic group E$_2$ in the inverse direction shows an enantiotropic nematic phase. On cooling the nematic phase one monotropic smectic phase appeared which exhibits a schlieren or fan-shaped texture. Owing to the metastable nature of this phase it was not possible to characterise it by X-ray diffraction and electro-optical studies. Hence, it has been designated as an unknown biaxial smectic phase SmC$_x$.

The nematic phase of compound **2-E$_2$** displays some unusual optical and electro-optical properties. Over the whole existence range of the nematic phase chiral domains of opposite handedness can be observed, although the molecules are achiral. Starting from the crossed position of the polariser and analyser, by slight decrossing chiral domains appear, as shown in Figure 3. The brightness of the (+) and (–) domains is reversed by changing the direction of the analyser. These domains can also be seen by illuminating the sample with circularly polarised light in the reflection mode of the microscope. Up to now, such behaviour has also been reported for a few monomeric banana-shaped liquid crystals [39, 40].

Furthermore, the nematic phase shows an unusual electro-optical response. On application of a relatively low a.c. field (1.2 V μm$^{-1}$; 22 Hz) to the planar-oriented nematic phase in a 6 μm polyimide-coated cell, fluctuating domains appear. These domains are of the Williams–Kapustin type, since their period, $d_{dom}$, corresponds to the cell thickness (6 μm). On applying higher fields and higher frequencies (3.3 V μm$^{-1}$; 120 Hz) to the planar-oriented nematic phase, domains with equidistant stripes parallel to the original orientation of the director $\boldsymbol{n_o}$ appear (longitudinal patterns, see Figure 4(a)). The period of these domains was found to be 10 μm, which is clearly greater than the sample thickness. On further increasing the voltage the domain period decreases, i.e. 7 μm at 6 V μm$^{-1}$, 5 μm at 10 V μm$^{-1}$. With increasing voltage (above 12 V μm$^{-1}$) the domain pattern is completely changed to a myeline-like texture with fine equidistant stripes ($d_{dom}$ decreases with increasing the voltage to 20 V μm$^{-1}$). Unusual effects are observed, such as transition between longitudinal and normal rolls (27 V μm$^{-1}$, 1 kHz; normal rolls, see

Table 1. Transition temperatures (°C), mesophase type, transition enthalpy values (kJ mol$^{-1}$), layer spacing $d$ (nm), tilt angle $\tau$ of the molecules (°) with respect to the layer normal in SmC phases and with respect to the normal to $a$ in $Col_{ob}$ phases, lattice parameters ($a$, $b$, $\gamma$) and $P_S$ values of the compounds **1–7**[a].

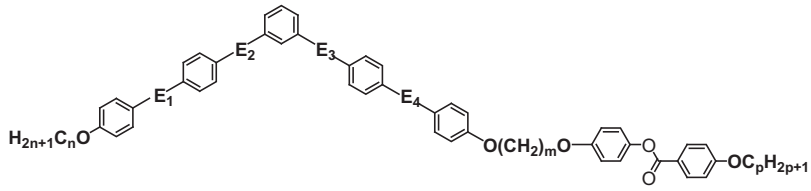


| Comp. | $n$ | $m$ | $p$ | $E$[d] | Transition temperatures (°C) $\Delta H$/kJ·mol$^{-1}$ | Phase type | Lattice parameters | | | | | $P_S$/nC cm$^{-2}$ |
|---|---|---|---|---|---|---|---|---|---|---|---|---|
| | | | | | | | $d$/nm | $\tau$/° | $a$/nm | $b$/nm | $\gamma$/° | |
| 1-$E_0$ | 12 | 3 | 6 | $E_0$ | Cr 150 ($Col_rP_{AF}$ 127) I<br>*65.7 24.0* | $Col_rP_{AF}$ | | – | 7.57 | 5.51 | 90.0 | 350 |
| 1-$E_2$ | 12 | 3 | 6 | $E_2$ | Cr 147 I<br>*54.4* | | – | – | – | – | – | – |
| 2-$E_0$ | 8 | 6 | 6 | $E_0$ | Cr 145 ($M_1$ 125 $SmC_sP_{FE}$ 130) N 151 I<br>*76.4 0.5 13.4 1.6* | N<br>$SmC_sP_{FE}$<br>$M_1$ | 5.80<br>–[c]<br>– | 26<br>–[c]<br>– | –<br>–[c]<br>– | –<br>–[c]<br>– | –<br>–[c]<br>– | 150<br>–[c]<br>– |
| 2-$E_2$ | 8 | 6 | 6 | $E_2$ | Cr 155 ($SmC_x$ 134) N 171 I<br>*70.0* 0.7 *2.9* | N<br>$SmC_x$ | –[c] | –[c] | | – | – | –[c] |
| 2-$E_3$ | 8 | 6 | 6 | $E_3$ | Cr 147 ($Col_x$ 127 $N_x$ 129) N 167 I<br>*55.8* –[b] *1.0 4.0* | N<br>$N_x$<br>$Col_x$ | | –[c] | –[c] | –[c] | –[c] | –[c] |
| 3-$E_0$ | 12 | 6 | 6 | $E_0$ | Cr 148.5 ($Col_x$ 125.5 N 145.5) I<br>*61.2 13.1 1.3* | N<br>$Col_x$ | | –[c] | –[c] | –[c] | –[c] | –[c] |
| 3-$E_1$ | 12 | 6 | 6 | $E_1$ | Cr 146 SmA 149 N 150 I<br>*48.5* –[b] *5.4* | N<br>SmA | 7.00 | | | | | – |
| 3-$E_2$ | 12 | 6 | 6 | $E_2$ | Cr 159 ($SmC_x$ 148) N 166 I<br>*69.8 0.04 3.1* | N<br>$SmC_x$ | –[c] | –[c] | | | | –[c] |
| 3-$E_3$ | 12 | 6 | 6 | $E_3$ | Cr 145 ($Col_x$ 130) N 161 I<br>*64.9* –[b] *2.6* | N<br>$Col_x$ | | –[c] | –[c] | –[c] | –[c] | –[c] |
| 3-$E_4$ | 12 | 6 | 6 | $E_4$ | Cr 140 ($Col_x$ 130) N 143 I<br>*54.1* –[b] *1.7* | N<br>$Col_x$ | | –[c] | –[c] | –[c] | –[c] | –[c] |
| 4-$E_0$ | 16 | 6 | 6 | $E_0$ | Cr 150 ($Col_x$ 126.5 N 142) I<br>*65.0* –[b] *1.4* | N<br>$Col_x$ | | –[c] | –[c] | –[c] | –[c] | –[c] |
| 4-$E_2$ | 16 | 6 | 6 | $E_2$ | Cr 160 ($SmC_x$ 144) SmA 163 N 164 I<br>*63.5* –[b] *0.5 5.3* | N<br>SmA<br>$SmC_x$ | 7.19<br>–[c] | –[c] | – | – | –[c] | –<br>– |
| 4-$E_3$ | 16 | 6 | 6 | $E_3$ | Cr 149 ($Col_x$ 133) N 158 I<br>*58.9* –[b] *2.9* | N<br>$Col_x$ | | –[c] | –[c] | –[c] | –[c] | –[c] |
| 5-$E_0$ | 12 | 6 | 12 | $E_0$ | Cr 140 ($Col_x$ 115.5 N 131) I<br>*86.3* –[b] *1.6* | N<br>$Col_x$ | | –[c] | –[c] | –[c] | –[c] | –[c] |
| 5-$E_2$ | 12 | 6 | 12 | $E_2$ | Cr 140 ($SmC_s$'$P_{AF}$ 131) $SmC_sP_{AF}$ 163 I<br>*88.5 8.5 11.7* | $SmC_sP_{AF}$<br>$SmC_s$'$P_{AF}$ | 6.19<br>6.10 | 24<br>32 | | | | 550<br>780 |
| 6-$E_0$ | 12 | 11 | 6 | $E_0$ | Cr 121 $Col_{ob}P_{FE}$ 132.5 I<br>*58.8 25.3* | $Col_{ob}P_{FE}$ | | 46 | 3.20 | 5.00 | 110.0 | 380 |
| 6-$E_1$ | 12 | 11 | 6 | $E_1$ | Cr 126 $USmC_aP_{AF}$ 130 I<br>*39.7 24.7* | $USmC_aP_{AF}$ | | 22 | 36.8 | 6.61 | 90.0 | 550 |
| 6-$E_2$ | 12 | 11 | 6 | $E_2$ | Cr 131 ($Col_x$ 128 N 129) I<br>*67.4 21.2 0.04* | N<br>$Col_x$ | | | –[c] | –[c] | –[c] | –[c] |
| 7-$E_0$ | 12 | 11 | 12 | $E_0$ | Cr 126 ($Col_rP_{AF}$ 121) I<br>*57.0 7.4* | $Col_rP_{AF}$ | | 29 | 16.06 | 6.76 | 90.0 | 450 |
| 7-$E_2$ | 12 | 11 | 12 | $E_2$ | Cr 133 ($Col_r$ 131) I<br>*85.2 30.3* | $Col_r$ | | – | 21.4 | 6.89 | 90.0 | – |

Notes: [a] Transition temperatures (°C) and enthalpy values (kJ mol$^{-1}$) were taken from the second differential scanning calorimetry (DSC) heating scans (10 K min$^{-1}$); values in parentheses indicate monotropic mesophases, in this case the transition temperatures and enthalpy values were taken from the first DSC cooling scans and the transition temperatures were checked by polarising microscopy; [b] the transition is not detectable on DSC and the transition temperature value is determined by polarising microscopy; [c] could not be determined due to rapid crystallisation of the sample; [d] the direction of the ester linking group $E_1$-$E_4$ which is opposite to the corresponding one in the reference structure $E_0$; [e] N: nematic phase; SmA: smectic A phase; SmC: smectic C phase; Col: columnar phase (r: rectangular, obl: oblique); M: non-classified mesophase; I: isotropic liquid. FE/AF: ferroelectric/antiferroelectric behaviour.

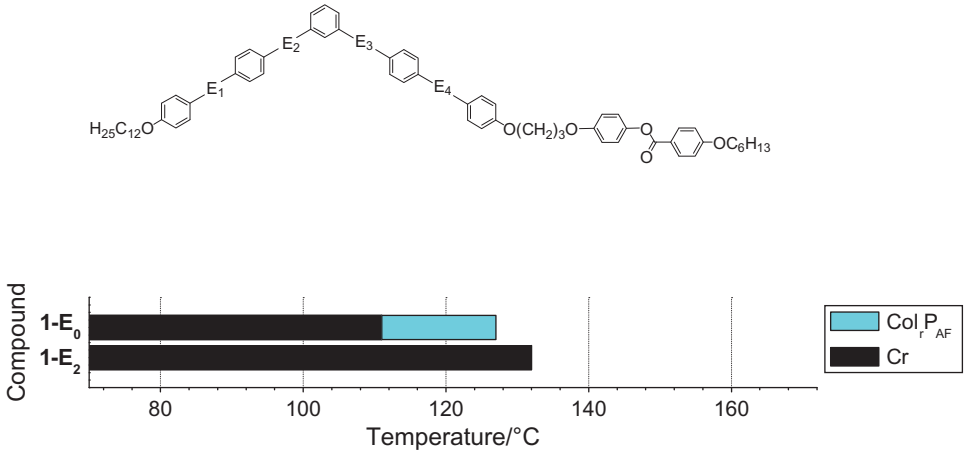


Figure 1. Mesophase behaviour and transition temperatures (°C) of compounds **1-E$_0$ and 1-E$_2$** taken from the first differential scanning calorimetry cooling scans (10 Kmin$^{-1}$).



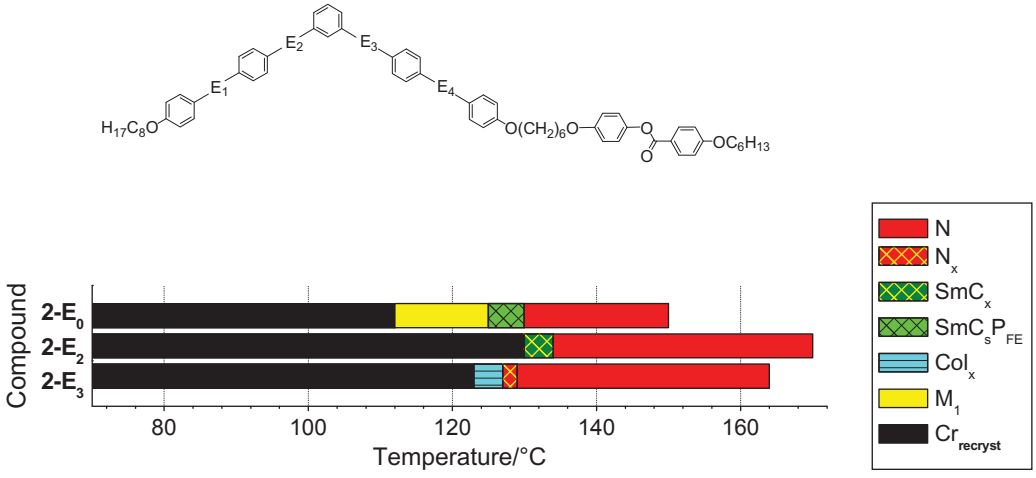


Figure 2. Mesophase behaviour of the dimers **2-E$_0$, 2-E$_2$, 2-E$_3$** on cooling.

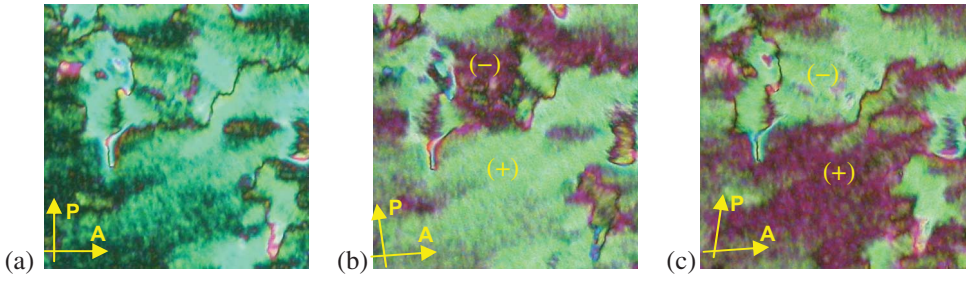


Figure 3. Optical photomicrographs of compound **2-E$_2$** in the nematic phase at 150°C in an ITO non-coated cell (cell thickness: 5 μm, at $U = 0$ V) observed under crossed polarisers (a) and by rotating one polariser by +15° (b) and by −15° (c) from the crossed position showing chiral (+) and (−) domains; the yellow arrows indicate the directions of the analyser and polariser.

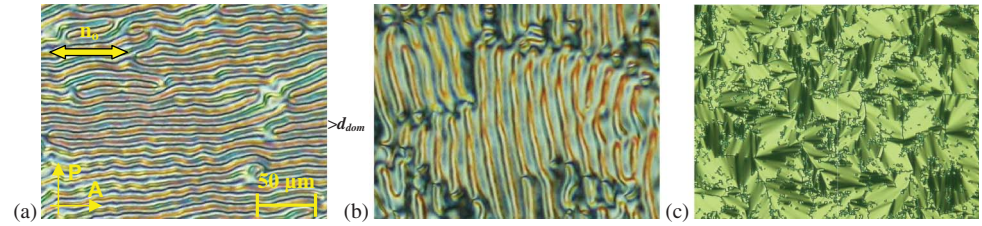


Figure 4. Field-induced texture changes of the nematic phase of compound **2-E$_2$** at 150°C in a 6 µm polyimide-coated ITO cell on application of an a.c. field: (a) 3.3 V µm$^{-1}$, 120 Hz; (b) 27 V µm$^{-1}$, 1 kHz; (c) 33 V µm$^{-1}$, 120 Hz; the black arrows in (a) mark the period of the domains which was found to be 10 µm and is clearly greater than the cell thickness 6 µm; the orientation of the initial director $\boldsymbol{n_o}$ is marked (colour version online).

Figure 4(b)), controlled by the excitation frequency. Details on such electroconvection behaviour in the nematic phase of the banana-calamitic dimer **3-E$_2$** have been reported by Heuer *et al.* [34, 36]. On application of a relatively high a.c. field (33 V µm$^{-1}$), the stripes disappear and an optical texture results which is reminiscent of a smectic fan-shaped texture, see Figure 4(c). This field-induced fan-shaped texture is observed over the whole existence region of the nematic phase. However, during the electro-optical experiments no polar switching was detected. If the electric field is removed, the smectic-like texture disappears and the texture of the planar-oriented nematic phase reappears. Similar electro-optical behaviour has been reported for the nematic phase of several monomeric bent-core compounds [39–41].

The isomer **2-E$_3$,** with the third ester linking group in the inverse direction, exhibits three mesophases which can be clearly distinguished by their textures and by DSC. According to its characteristic texture the high-temperature phase can be assigned as nematic. This nematic phase shows typical marbled, homeotropic and/or planar textures (see Figure 5(a)) and forms chiral domains of opposite handedness over the whole temperature range. The transition from the isotropic state to the nematic one at 164°C has an enthalpy change of 4.0 kJ mol$^{-1}$. On cooling the nematic phase a clear change in the optical texture occurs below 129°C, which is accompanied by a rather low transition enthalpy (1.0 kJ mol$^{-1}$). The long-range director fluctuations which are characteristic of a nematic phase disappear and a fine structured fan-like texture develops, see Figure 5(b). It is remarkable that this fan-like texture does not show typical focal-conic defects. On the other hand, the texture of homeotropically oriented regions remains unchanged below 129°C, the director fluctuations disappear and some oily strikes become visible. The occurrence of the

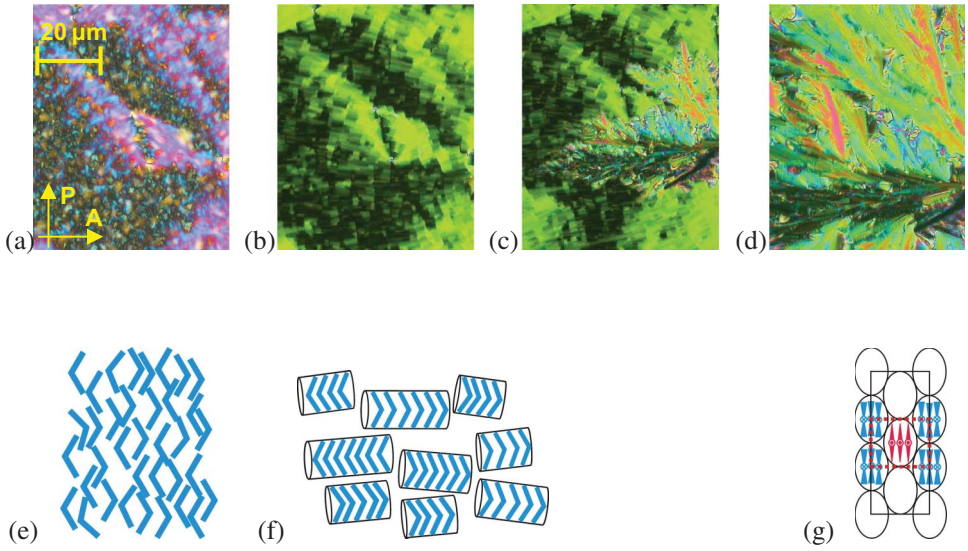


Figure 5. (a–d) Textures of the mesophases of compound **2-E$_3$** formed on cooling: (a) planar texture of the nematic phase at 163°C; (b) fan-like texture of the $N_x$ phase at 128°C; (c) dendritic growing of a mosaic texture of the $Col_x$ phase in the fan-like texture of the $N_x$ phase at 127°C; (d) mosaic texture of the $Col_x$ phase at 126°C; (e–g) proposed models for the nematic (e), $N_x$ (f) and $Col_r$ (g) phases by analogy to Schröder *et al.* [42] (colour version online).

homeotropic texture is an indication of a uniaxial phase. On cooling from this phase, at 127°C a dendritic growth of the texture can be observed, which transforms into a mosaic-like texture suggesting a columnar phase, see Figure 5(c) and (d).

X-ray diffraction (XRD) measurements have been performed on samples of compound **2-E$_3$** aligned in a magnetic field of about 1 T. The results confirm that the high-temperature phase is nematic. The X-ray pattern shows a diffuse dumbbell-like scattering in the small-angle region, and a diffuse wide-angle scattering located around the equator (at 155°C, Figure 6 (a) and (b)). The diffuse small-angle scattering in the nematic phase can be attributed to cybotactic groups representing fluctuating arrays of molecules with a short-range smectic-like order. Surprisingly, this pattern did not show significant changes at the transition to the low-temperature $N_x$ phase (at 128°C, Figure 6(c) and (d)), although the fan-like texture indicates the existence of a smectic-like phase (see Figure 5(d)). The distribution of the wide-angle scattering along $\chi$ and the corresponding $\theta$-scan of the diffraction pattern in the N and $N_x$ phases are shown in Figure 6 (e) and (f). The experimental results, shown in Figure 6, prove that both nematic phases N and $N_x$ cannot be clearly distinguished by X-ray methods.

Due to the metastable nature of the low-temperature columnar phase it was not possible to characterise it by XRD and electro-optical studies. Hence, it has been designated as an unknown columnar phase ($Col_x$).

A similar phase sequence N–$N_x$–$Col_r$ has already been reported by Schröder *et al.* [42] for bent-core mesogens with a central N-benzoylpiperazine fragment. Based on the experimental results, this unusual behaviour can be explained by the following structural model. In the N phase the molecules adopt only an orientational order with respect to the averaged molecular long axes (see Figure 5(e)). On the other hand, in the $N_x$ phase (see Figure 5(f)) the molecules are stacked along the bent direction in bundles of undefined length. Between the bundles (aggregates) only a short-range positional order exists, giving rise to the diffuse scattering. In order to prevent a macroscopic polarisation, neighbouring bundles should be aligned anti-parallel. On further cooling the lateral distances of the bundles are fixed and the structure passes over into a two-dimensional columnar structure (see Figure 5(g)). That means the $N_x$ phase can be regarded as the precursor to the following low-temperature $Col_x$ phase.

### *3.3 Compounds 3-E$_0$, 3-E$_1$, 3-E$_2$, 3-E$_3$ and 3-E$_4$ ($n = 12$; $m = 6$; $p = 6$)*

In comparison to series **2**, in series **3** the spacer ($m = 6$) and the hexyloxy group at the calamitic unit ($p = 6$) are unchanged, but the length of the hydrocarbon chain attached to the bent-core moiety is increased to

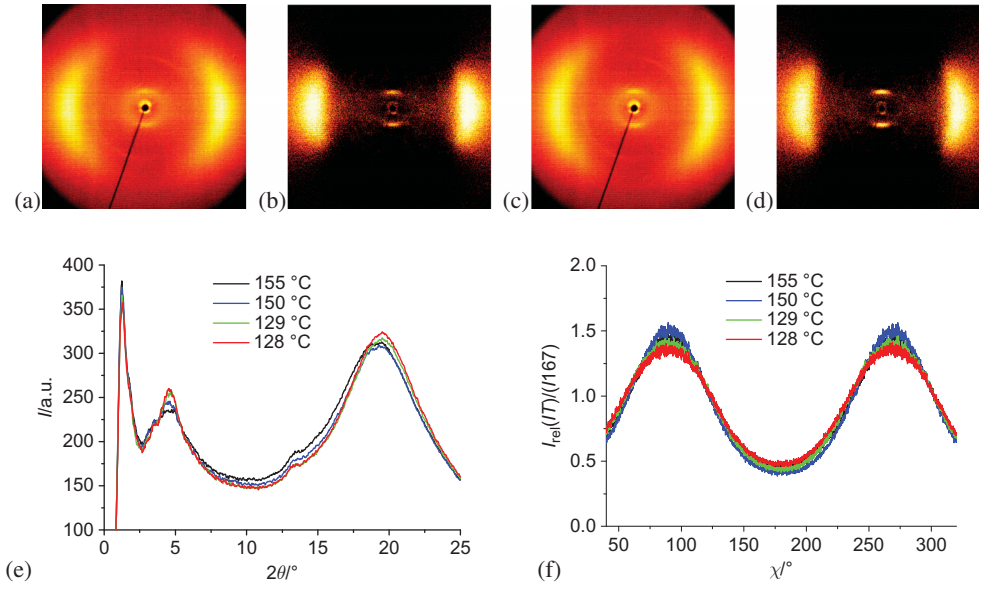


Figure 6. X-ray diffraction patterns of a sample of compound **2-E$_3$** aligned in the magnetic field on cooling: (a), (b) patterns of the nematic phase at 155°C; (c), (d) patterns of the $N_x$ phase at 128°C: (a), (c) original scattering; (b), (d) the same patterns, but the scattering of the isotropic liquid has been subtracted; (e) $\theta$-scans of the diffraction patterns in the N and $N_x$ phases; (g) distribution of the wide-angle scattering along $\chi$ in the nematic phase (black and blue lines) and in the $N_x$ phase (green and red lines) ($I_{rel} = I(T)/I$)(167°C, isotropic liquid) (colour version online).

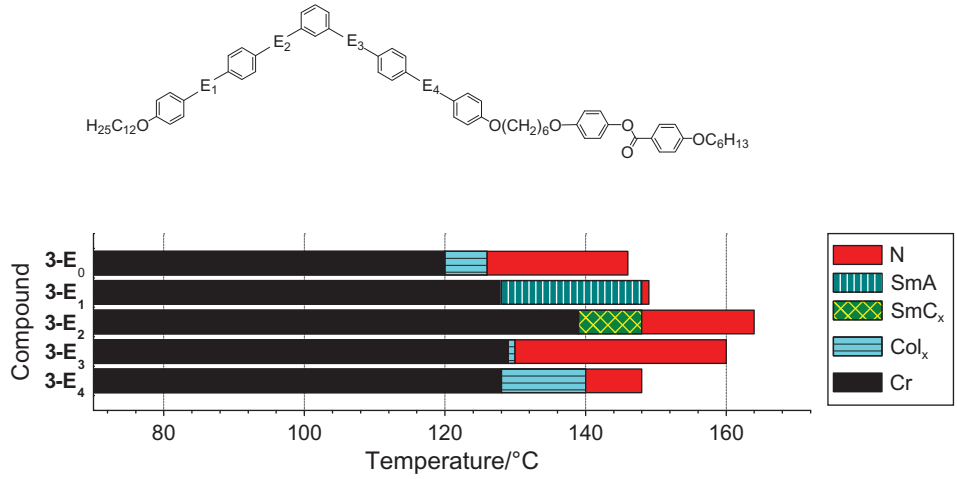


Figure 7. Mesophase behaviour of the dimers **3-E$_0$** and **3-E$_{1–4}$** on cooling.

dodecyloxy ($n = 12$). In addition, the directions of all four linking groups $E_1$ to $E_4$ have been systematically reversed step by step, giving the isomers **3-E$_{1–4}$**. Whereas the reference compound **3-E$_0$** exhibits a monotropic nematic and a monotropic columnar phase only, all dimers **3-E$_{1–4}$** having one reversed carboxylic group exhibit, beside a low-temperature phase, an enantiotropic nematic phase, however, with very different ranges of existence, see Figure 7. The clearing temperatures vary between 143°C (**3-E$_4$**) and 166°C (**3-E$_2$**) and increase in the sequence: $T(E_4) < T(E_0) < T(E_1) < T(E_3) < T(E_2)$.

The nematic phase of the dimer **3-E$_1$** exists over a very small temperature interval (~1 K), the texture of which is shown in Figure 8(a). On cooling a smectic phase appears, characterised by a homeotropic or fan-shaped texture, see Figure 8 (b) and (c). The X-ray pattern of the smectic phase at 140°C obtained from an aligned sample shows a diffuse outer scattering with the maxima located on the equator and Bragg-reflections on the meridian, from which a layer spacing of 7.0 nm is calculated, see Figure 8 (d) and (e). This finding indicates a SmA phase. In addition, no electro-optical response could be observed on applying an a.c. or d.c. field.

The knowledge of the layer spacing, *d,* of 7.0 nm in the SmA phase could encourage a discussion on the packing of the banana-calamitic molecules. A calotte model of the dimer **3-E$_1$** gives a similar value for *L* of 6.93 nm in its most stretched conformation, see Figure 9(a). This is a hint at a monolayer packing; a strong intercalation of the different molecular fragments can most probably be excluded. However, a determination of the molecular shape of liquid crystalline dimers is not simple, as already discussed by Imrie and Luckhurst [6]. This is especially true for large molecules with an unconventional shape. However, for compound **6-E$_1$** (see later in this section), a comparison of the lattice parameters with the corresponding calotte model would favour a more hockey-stick like or bent conformation, as shown in Figure 9(b). Also in this case an intercalation can be excluded in all probability. However, it should be stressed again: since the molecular conformations of the dimers are unknown and a lot of different molecular shapes can be assumed, the construction of such a structural model is rather speculative.

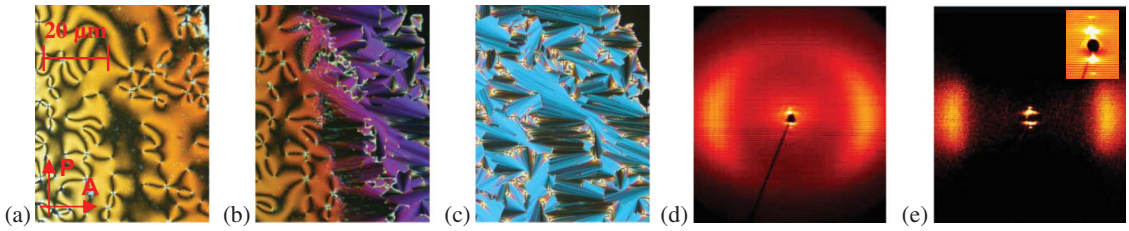


Figure 8. Textures of the mesophases of compound **3-E$_1$** on cooling: (a) schlieren texture of the nematic phase at 149°C; (b) fan-shaped texture of the SmA phase growing from the schlieren texture of the nematic phase at 148.5°C; (c) fan-shaped texture and homeotropic region of the SmA phase at 145°C; X-ray diffraction (XRD) patterns of a surface-aligned sample in the SmA phase at 140°C; (d) original pattern; (e) the same XRD pattern, but the intensity of the isotropic liquid is subtracted; the inset shows the small-angle region.

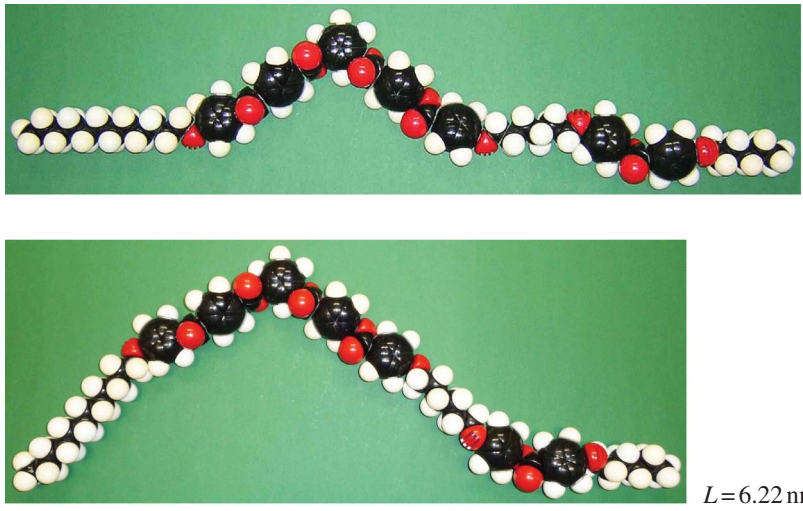


Figure 9. CPK models of molecule **3-E$_1$** showing two possible conformations of the banana-calamitic dimer.

The dimer **3-E$_2$** exhibits a nematic phase and a monotropic smectic phase. The reversal of the direction of the second ester connecting group results in an increase of the clearing point by 20 K in comparison with the isomer **3-E$_0$**. The nematic phase shows typical marbled and homeotropic textures and chiral domains of opposite handedness over the whole temperature range. On cooling the homeotropic texture of the nematic phase below 148°C, a transition into a weakly birefringent, fluctuating schlieren texture takes place, indicating a biaxial smectic phase $SmC_x$. This transition is accompanied by a very small calorimetric peak (0.04 kJ mol$^{-1}$). The low-temperature smectic phase crystallises very fast, and so we could not distinguish between a polar and non-polar phase, respectively. It should be mentioned that extensive physical measurements were performed using compound **3-E$_2$** [34, 36].

For the compounds **3-E$_3$** and **3-E$_4$**, textural and calorimetric investigations provide evidence for the existence of enantiotropic nematic and monotropic columnar phases ($Col_x$). Further electro-optical experiments and XRD measurements were not successful due to rapid crystallisation.

### *3.4 Compounds 4-E$_0$, 4-E$_2$, and 4-E$_3$ ($n = 16$; $m = 6$; $p = 6$)*

Series **4-E** is the continuation of series **3-E** and **2-E**: the spacer length $m = 6$ and the hexyloxy group ($p = 6$) at the calamitic part remain constant; however, the length of the alkyloxy chain attached to the bent-core unit is increased to hexadecyloxy ($n = 16$). The transition behaviour is given in Table 1 and Figure 10.

The dimers **4-E$_0$** and **4-E$_3$** present a similar mesophase sequence. Below a relatively broad nematic range a columnar phase exists which cannot be characterised in detail due to fast recrystallisation. The dimer **4-E$_2$** exhibits two enantiotropic mesophases, a nematic and a

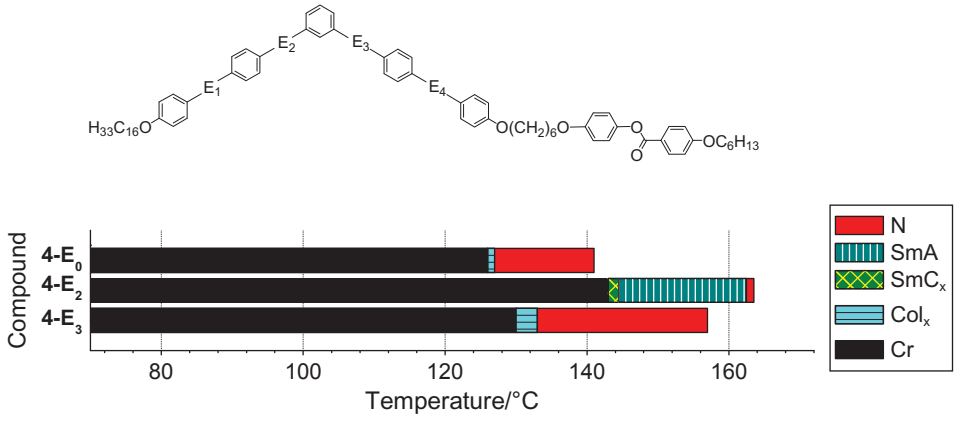


Figure 10. Mesophase behaviour of the dimers **4-E$_0$**, **4-E$_2$** and **4-E$_3$** on cooling.

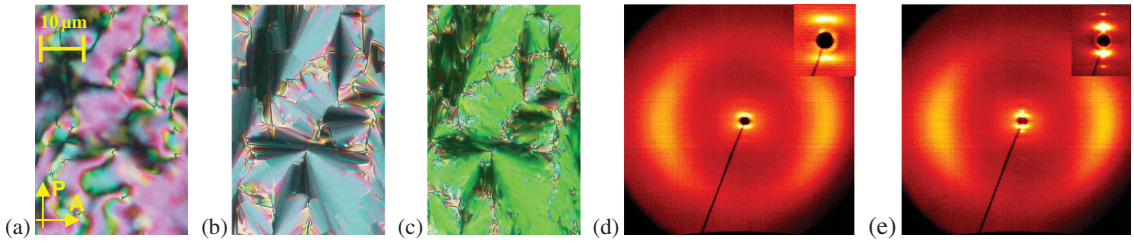


Figure 11. Textures of the mesophases of compound **4-E$_2$** on cooling: (a) nematic phase at 163°C; (b) SmA phase at 148 °C; (c) SmC$_x$ phase at 144°C; X-ray diffraction patterns of a sample of compound **4-E$_2$** aligned in the magnetic field; (d) pattern of the nematic phase at 163°C; (e) pattern of the SmA phase at 150°C; the inset shows the small-angle region (colour version online).

high-temperature smectic phase, and in addition a monotropic low-temperature smectic phase. On cooling the nematic phase (texture see Figure 11(a)), a homeotropic texture as well as a smooth fan-shaped texture was observed, which is a typical feature of a SmA phase (see Figure 11(b)). On lowering the temperature (below 144°C), the homeotropic regions transform into a weakly birefringent fluctuating schlieren texture, indicating a biaxial phase. On cooling the smooth fan-shaped texture a broken fan-shaped texture appears (see Figure 11(c)). Rapid crystallisation prevents detailed investigations on this biaxial low-temperature smectic phase, which was designated as a SmC$_x$ phase.

X-ray measurements on compound **4-E$_2$** at 163°C show the typical scattering of a nematic phase (see Figure 11(d)). The measurements at 150°C confirm the presence of a SmA phase. The X-ray pattern shows strong small-angle reflections from which a layer spacing of 7.19 nm could be determined (see Figure 11(e)) and two distinct diffuse wide-angle halos with the maximum at 0.50 nm in a direction normal to the layer reflections.

The SmA phase does not show a polar electro-optical response. However, under a sufficiently high electric field (about 40 V µm$^{-1}$), the SmA texture (see Figure 12(a)) can be transformed into an optically biaxial texture. This field-induced transition can be observed up to 4 K above the SmC$_x$–SmA transition temperature (see Figure 12(b)).

If the field is switched off the original fan-shaped texture of the SmA phase reappears. The field-induced phase can be assigned as a SmC$_x$P$_{AF}$ phase because an antiferroelectric switching can be measured, as shown in Figure 12(c). That means the transition temperature for

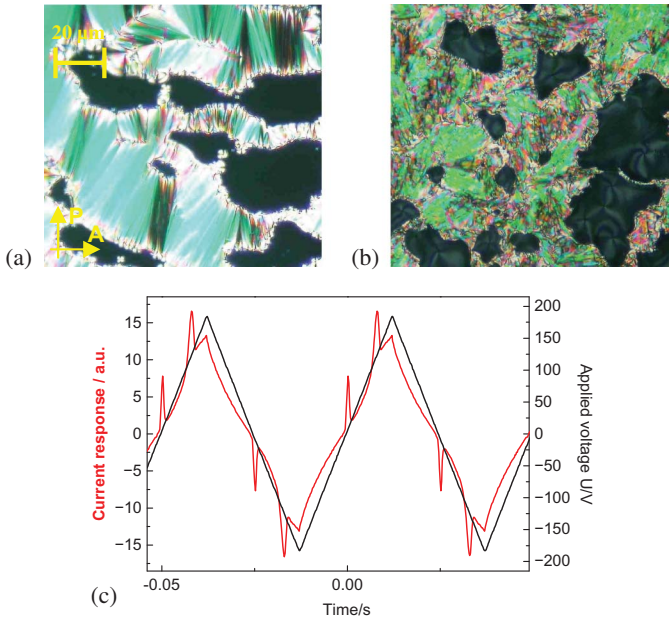


Figure 12. Compound **4-E$_2$**: Electro-optical investigations on the field-induced SmC$_x$P$_{AF}$ phase formed from the SmA phase under a d.c. electric field at 147°C in a 5 µm non-coated ITO cell: (a) $U = 0$ V; (b) $U = \pm 200$ V; (c) AF switching current response obtained by applying a triangular-wave voltage ($U = 400$ V$_{pp}$, $f = 20$ Hz, $R = 5$ kΩ, $T = 147$°C, $P_S = 450$ nC cm$^{-2}$) (colour version online).

$SmC_x$ to SmA can be increased by the application of a sufficiently high electric field. On applying a field of 40 V $\mu m^{-1}$ the increase of the transition temperature was found to be about 4 K. This effect may be connected with the existence of polar clusters in a short-range order region already in the non-polar SmA phase.

A similar field-induced enhancement of the transition temperature between polar and non-polar phases was reported in the literature for a few monomeric bent-core mesogens, especially for the phase transitions $SmCP_{AF}$–SmA, $SmCP_{AF}$–isotropic liquid, crystalline-polar–isotropic [43–47].

### 3.5 *Compounds 5-$E_0$ and 5-$E_2$ ($n = 12$; $m = 6$; $p = 12$)*

In the banana-calamitic dimers **5-E** both mesogenic units are connected by an even-numbered spacer ($m = 6$), the same as that used in series **2-E** to **4-E;** however, both terminal chains have the same length: $n, p = 12$. Such symmetric substitution has a clear influence on the mesophase behaviour. Whereas compound **5-$E_0$** exhibits a nematic–columnar dimorphism, for compound **5-$E_2$** with a reversed carboxylic group in position 2, the type and sequence of phases is changed, see Figure 13. Interestingly, compound **5-$E_2$** is the first banana-calamitic dimer with an *even*-methylene spacer which does not form a nematic phase.

Furthermore, the reversal of the second ester linking group results in a stabilisation of the mesophase: the clearing temperature of compound **5-$E_2$** is 23 K higher than that of the corresponding **5-$E_0$**-isomer. Compound **5-$E_2$** forms two smectic phases which were identified according to their characteristic schlieren textures. The high-temperature smectic phase exhibits a schlieren texture with singularities of $S = \pm 1$, $S = \pm 1/2$ and $S = \pm 3/2$ (indication of a tilted smectic mesophase) and a birefringent smooth fan-shaped texture which points to an anticlinic SmC phase. On further cooling, a monotropic smectic phase appeared, showing either a broken-fan-shaped texture or a low-birefringent *grainy* non-specific texture, which is not a homeotropic one (see Figure 14).

X-ray measurements performed at 155°C and at 126°C confirm the presence of two SmC phases designated as SmC and SmĆ with molecules tilted with respect to the layer normal and very similar patterns for both phases (see Figure 15). The layer spacing is almost independent of temperature, including the transition from the high-temperature $SmC_s$ ($d = 6.19$ nm) to the low-temperature $SmC_s$' phase ($d' = 6.10$ nm). An average tilt angle of the molecular long axis with respect to the layer normal can be calculated from the position of the maxima for the outer diffuse scattering in the SmC phase ($\tau = 24°$)

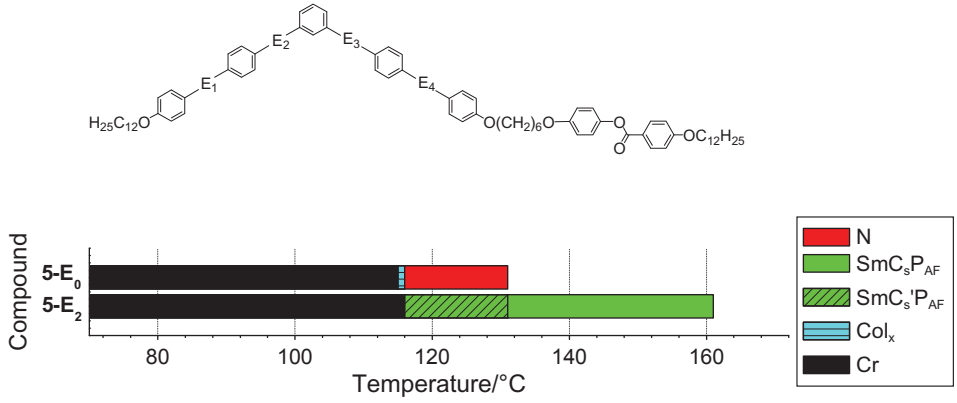


Figure 13. Mesophase behaviour of the dimers **5-$E_0$** and **5-$E_2$** on cooling.

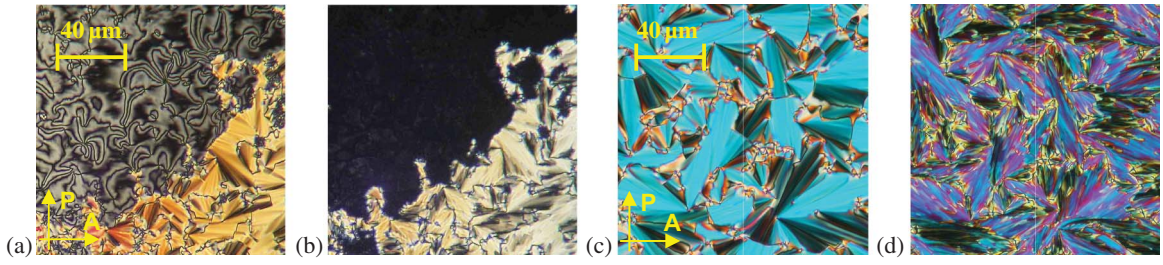


Figure 14. Compound **5-$E_2$**: (a), (c) Textures of the high-temperature $SmC_sP_{AF}$ at 160°C; (b), (d) of the low-temperature $SmC_s'P_{AF}$ phase at 130°C (colour version online).

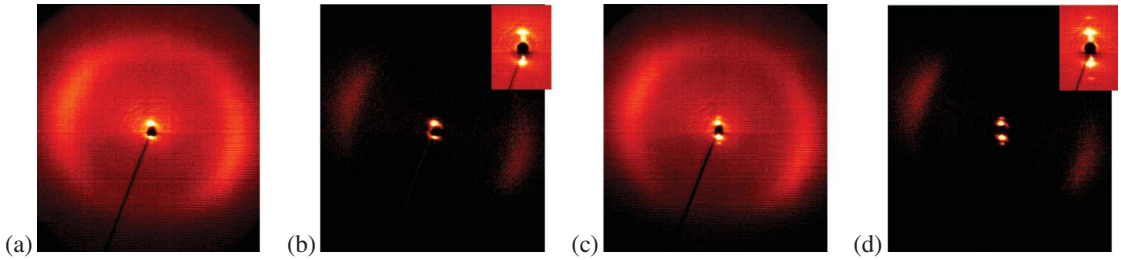


Figure 15. X-ray diffraction patterns of a surface-aligned sample of compound **5-E$_2$** on cooling; (a), (b) $SmC_s$ phase at 155°C; (c), (d) $SmC_s$' phase at 126°C; (a), (c) original wide-angle patterns; (b), (d) the same patterns, but the scattering intensity of the isotropic liquid is subtracted; the insets show the small-angle region.

and in the SmC' phase ($\tau' = 32°$). The effective molecular length calculated for SmC is $L_{eff} = d/\cos\tau = 6.78$ nm and for SmC' is $L_{eff}' = 7.19$ nm. The intensity distribution of the outer diffuse scattering indicates a synclinic tilt of the molecules in adjacent layers in both phases, because the maxima in the upper left and the lower right quadrant of the patterns are significantly stronger than those in the other two quadrants [45]. It is remarkable that this result is in contradiction with the textural investigations for the high-temperature $SmC_s$ phase, which point to an anticlinic mesophase.

Electro-optical measurements give evidence for an antiferroelectric (AF) ground state in both $SmC_s$ phases ($P_S = 550$ nC cm$^{-2}$ for the $SmC_sP_{AF}$ phase and $P_S = 780$ nC cm$^{-2}$ for the $SmC_s'P_{AF}$ phase). The two SmCP phases show a similar electro-optical switching. The two synclinic $SmC_s$ phases form a smoother fan-like texture under the electric field which does not depend on the polarity of the applied field. If the field is removed the texture remains almost unchanged; only the birefringence is slightly changed, see Figure 16. This finding would suggest that the synclinic organisation of the ground-state structure is

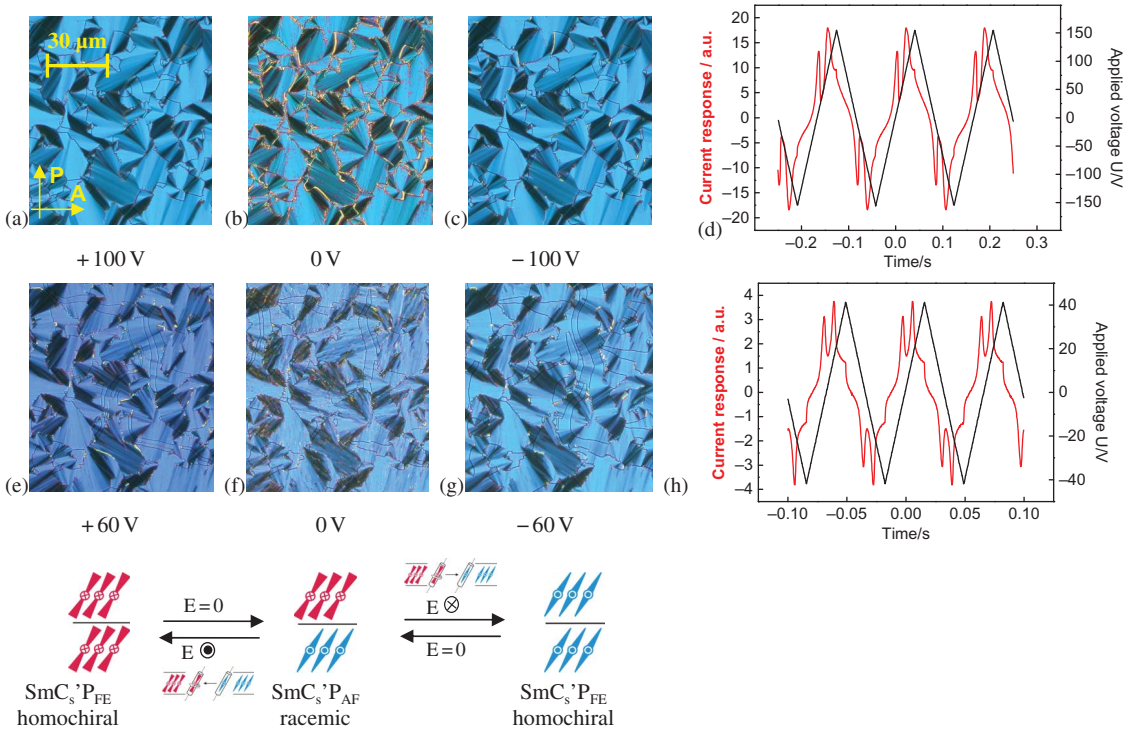


Figure 16. Electro-optical investigations of compound **5-E$_2$** under a d.c. electric field in a 5 µm non-coated ITO cell: (a–d) high-temperature $SmC_sP_{AF}$ phase at 155°C; (a),(c) $U = \pm 100$ V and (b) $U = 0$ V; (d) antiferroelectric (AF) switching current response obtained by applying a triangular-wave voltage ($U = 315$ V$_{pp}$, $f = 5$ Hz, $R = 5$ kΩ, $P_S = 550$ nC cm$^{-2}$); (e–h) low-temperature $SmC_s'P_{AF}$ phase at 126°C: (e), (g) $U = \pm 60$ V and (f) $U = 0$ V; (h) AF switching current response ($U = 90$ V$_{pp}$, $f = 8$ Hz, $R = 5$ kΩ, $P_S = 780$ nC cm$^{-2}$); models of the molecular organisation during the switching process are sketched below the textures: FE states (a), (c), (e), (g) and AF ground state (b), (f).

not significantly changed by the field and the switching takes place by rotation around the long axis.

It should be noted that this switching process gives rise to a change of the superstructural chirality from racemic at zero voltage to homogeneously chiral under the applied field, and the change of the sign of the applied field switches between the enantiomeric chiral states.

### *3.6 Compounds 6-E$_0$, 6-E$_1$ and 6-E$_2$ (n = 12; m = 11; p = 6)*

The spacer of the following two series is increased from $m = 6$ to $m = 11$; this means that both mesogenic units are connected by an odd-numbered spacer. A relatively short hexyloxy group is attached ($p = 6$) to the calamitic moiety, and the bent-core part bears a dodecyloxy substituent ($n = 12$).

The columnar phases of the reference material **6-E$_0$** and of the compound **6-E$_2$** exhibit a comparable mesophase stability, see Figure 17. On cooling the isotropic liquid of compound **6-E$_2$**, however, a small existence range of a nematic phase could be observed before the columnar phase appears. This is of interest, because it is the only nematic phase formed by a banana-calamitic dimer under study having an odd-numbered spacer. The nematic phase shows typical schlieren (see Figure 17(a)) and/or marbled and homeotropic textures. On cooling the nematic phase a dendritic growth of the columnar phase can be observed which then leads to mosaic-like regions (see Figure 18(b) and (c)). Electro-optical experiments and XRD measurements were not successful because of the early crystallisation.

The compound **6-E$_1$** shows an enantiotropic mesophase with some peculiar textural features (see Figure 19(a)–(e)). On cooling the isotropic liquid, this phase grows as dendritic nuclei or as spiral nuclei which coalesce to a variety of optical textures such as focal conics, banana-leaf-like regions, and circular domains together with ribbon-like and spherulitic textures. The growth of the phase suggests a mesophase belonging to the B$_7$ family [48].

The XRD pattern of a surface-aligned sample of compound **6-E$_1$** is characterised by sharp Bragg-reflections in the small-angle region and a diffuse scattering in the wide-angle region with a maximum at 0.46 nm, indicating a liquid-like lateral arrangement of the molecules within the layers (see Figure 20(a)). The

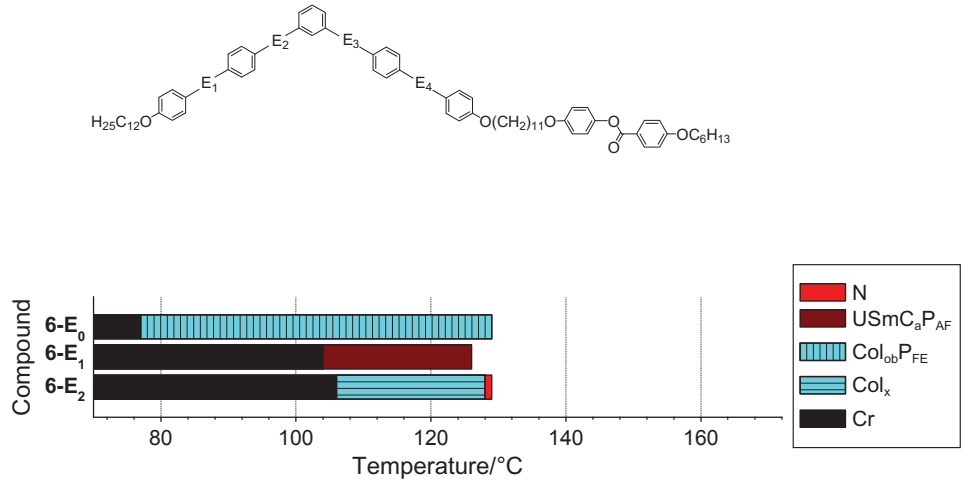


Figure 17. Mesophase behaviour of the dimers **6-E$_0$**, **6-E$_1$** and **6-E$_2$** on cooling.

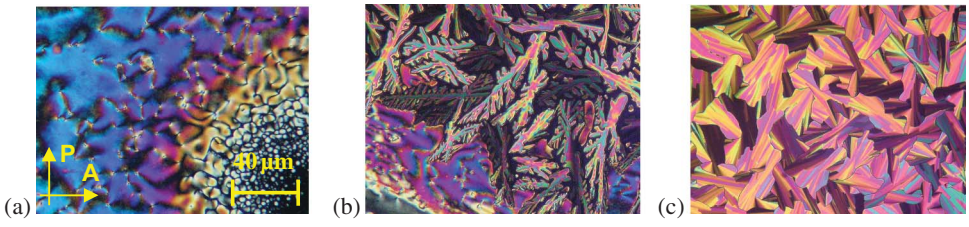


Figure 18. Textures of the mesophases of compound **6-E$_2$** on cooling: (a) nematic phase at 129 °C; (b) growth of the dendritic domains of the Col$_x$ phase on cooling from the nematic phase (lower left of the micrograph) at 128 °C; (c) the mosaic texture of the Col$_x$ phase at 120 °C (colour version online).

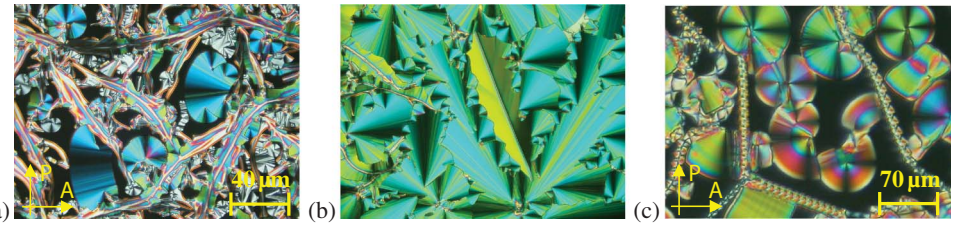


Figure 19. Textures of the mesophase of compound **6-E$_1$** observed on cooling from the isotropic state. (a), (b) 6 µm polyimide-coated cell; (c) 5 µm non-coated cell.

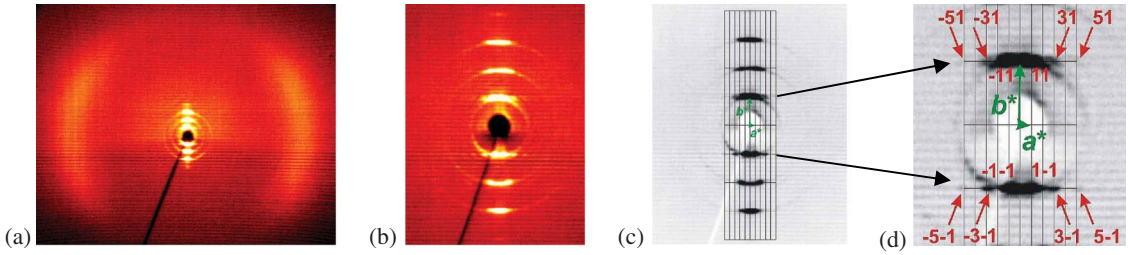


Figure 20. X-ray diffraction patterns of a surface-aligned sample of compound **6-E$_1$** in the USmC$_a$ phase at 120°C: (a) wide-angle pattern; (b) pattern of the small-angle region; (c) reciprocal lattice for the observed reflections; (d) close-up of the reciprocal lattice with indices for the observed *h*1 and *h*-1 reflections.



layer reflections and their satellites of weak intensity are arranged in lines parallel to the equator. They can be indexed on a centred rectangular 2D lattice, with the lattice parameters $a = 36.8$ nm and $b = 6.6$ nm (see Figure 20(b)–(d)). These features and the missing *h*0 reflections on the equator of the pattern (suggesting a nearly sinusoidal modulation of the electron density in direction *a* [50]) are typical for an undulated smectic structure. Therefore, this phase is given a preliminary assignment as an undulated smectic phase (USmC$_a$ phase) with a layer spacing of 6.6 nm and an undulation period of 36.8 nm. From the $\chi$-scan of the wide-angle region we estimated a tilt angle of the molecules with respect to the *b*-axes of the real lattice of 22°.

In addition to the structural features, the electro-optical behaviour is also particularly interesting. Under a triangular-wave voltage, AF switching could be observed for the USmC$_a$P$_{AF}$ phase, see Figure 21(d). The calculated value of the spontaneous polarisation is about 550 nC cm$^{-2}$ and increases on decreasing temperature. This can be explained by a reduction of the polar order at higher temperature, possibly due to the diminished barriers for the rotation around the molecular long axis. On cooling the isotropic liquid, under a d.c. voltage of 50 V circular domains were obtained (Figure 21(a)–(c)). The characteristic feature is the appearance of extinction crosses which are aligned along the direction of the crossed polarisers, indicating that the molecules adopt an anticlinic organisation. The field-induced circular domains do not change on reversal of the field. However, no relaxation of the extinction crosses could be seen on removing the applied field, apart from a small change in the birefringence (see Figure 21(b)). This means that the position and tilt of the molecules remains unchanged during the switching process, which can be explained by a polarisation reversal that takes place by rotation around the molecular long axes.

The textural features, the electro-optical behaviour, but especially the XRD pattern prove that the mesophase of compound **6-E$_1$** can be assigned as a B$_7'$ phase. According to Coleman *et al.* [49], the modulated layer structure formed by bent-core molecules in the B$_7'$ phase can be generated by splayed polarisation with domains of alternating tilt and polarisation periodically arranged in order to escape from a macroscopic polar order.

### *3.7 Compounds 7-E$_0$ and 7-E$_2$ ($n = 12$; $m = 11$; $p = 12$)*

Defining the odd-numbered spacer with $m = 11$, in the compounds **7-E** the two terminal chains have the same length: $n, p = 12$. As shown in Figure 22, both compounds **7-E$_0$** and **7-E$_2$** exhibit a rectangular columnar phase. Cooling the isotropic liquid of compound **7-E$_2$**, a dendritic growth could be observed with a birefringent texture containing sharp lines and leaf-like patterns (see Figure 23(a)), mosaic-like regions, and low-birefringent focal conic regions. As for compound

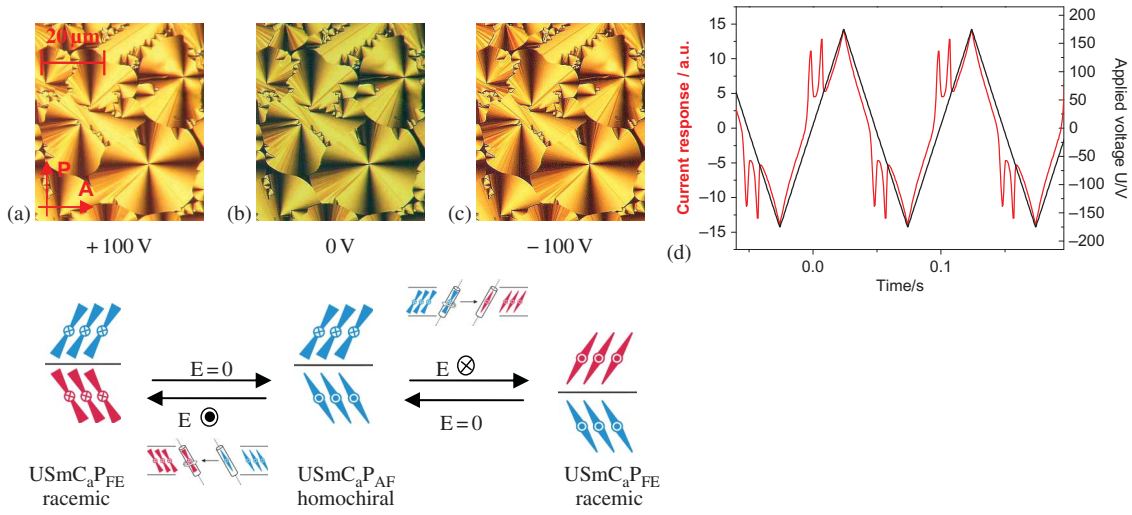


Figure 21. Electro-optical investigations on the USmC$_a$P$_{AF}$ phase of compound **6-E$_1$** under a d.c. electric field at 120°C in a 5 µm non-coated ITO cell: (a),(c) $U = \pm$ 100 V and (b) $U = 0$ V; (a–c), lower part of the figures, proposed models of the organisation of the molecules in the ribbons in the ferroelectric state (a), (c) and in the antiferrolelectric (AF) ground state (b); (d) AF switching current response obtained by applying a triangular-wave voltage ($U = 353$ V$_{pp}$, $f = 10$ Hz, $R = 5$ kΩ, $T = 120$°C, $P_S = 550$ nC cm$^{-2}$). In the schematic model, only the bent-core parts of the dimers are sketched because the calamitic moieties are not of importance for the electro-optical behaviour under discussion.



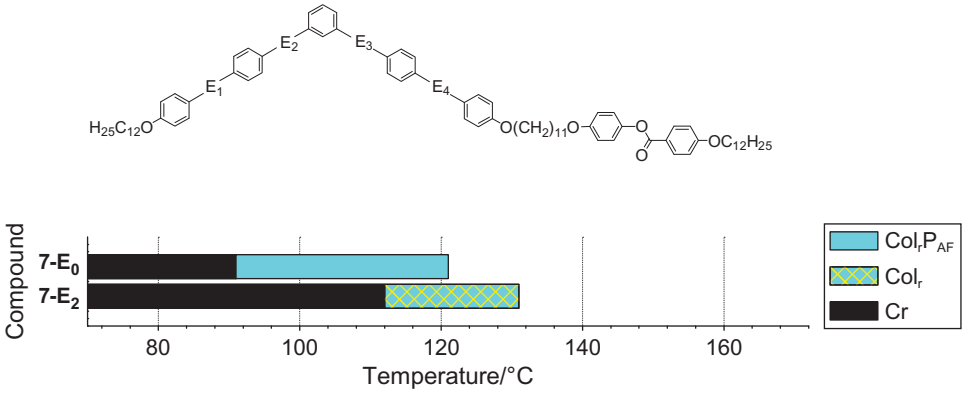


Figure 22. Mesophase behaviour of the dimers **7-E$_0$** and **7-E$_2$** on cooling.

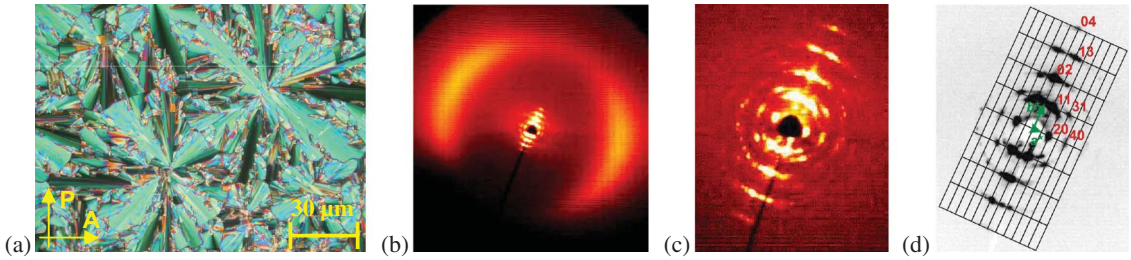


Figure 23. The Col$_r$ phase of compound **7-E$_2$**: (a) texture at 126°C in a 6 µm polyimide-coated ITO cell; (b–d) X-ray diffraction patterns of a surface-aligned sample at 126°C; (b) wide-angle pattern; (c) pattern of the small-angle region; (d) reciprocal lattice with *hk* values for the observed reflections.

**6-E$_1$** the XRD patterns of a surface-aligned sample are characterised by a diffuse scattering in the wide-angle region and sharp Bragg-reflections in the small-angle region (see Figure 23(b)–(d)), which can be indexed on a centred rectangular 2D lattice with the lattice parameters $a = 21.4$ nm, $b = 6.89$ nm. However, the

patterns of **6-E$_1$** show strong *h*0 reflections on the equator (see Figure 23(d)), a clear indication of a non-sinusoidal modulation of the electron density along *a*; hence this phase should not be called undulated, but it is a rectangular columnar phase ($Col_r$) with a rather large number of molecules in blocks with a width of 21.4 nm. Remarkably, for this compound no electro-optical response can be observed up to a voltage of about 400 $V_{pp}$ using a 5 μm-thick cell, the maximum voltage attainable from our experimental set-up. The reversal of the second ester linking group results in a mesophase stabilisation by 10 K in comparison to **7-E$_0$**, a loss of the antiferroelectricity and an increase in the lattice parameter *a*.

## 4. Discussion

To summarise the results, different aspects are of interest. A discussion of the chemical structure–property relationships results in the following: banana-calamitic dimers are suitable materials for studying the boundary between bent-core and calamitic compounds. This is shown by the existence of phase sequences combining nematic and/or SmA phases (characteristic for classical rod-like mesogens) with polar columnar and/or polar smectic phases (typical for bent-core mesogens). Compounds with an even-numbered spacer (**2-E** to **5-E**) exhibit higher clearing temperatures than those with an odd-numbered spacer (**1-E, 6-E, 7-E**), as expected. This means that also for banana-calamitic dimers the molecules with an even number of single units in the spacer should have a more stretched shape. Nearly all of these even-numbered dimers exhibit a nematic phase as a high-temperature phase with one exception. Two polar SmC phases are formed by compound **5-E$_2$**, symmetrically substituted at both terminal positions with dodecyloxy groups. Both phases, showing a synclinic tilt of the molecules in an AF layer arrangement, could be completely characterised. To the best of our knowledge such a $SmC'_sP_{AF}$–$SmC_sP_{AF}$ sequence has not been previously described for bent-core mesogens. Remarkably, the switching mechanism on applying an electric field is the same in these two SmCP phases, which is in contrast to the electro-optical behaviour of the two SmCP phases of a compound exhibiting the reentrant behaviour $SmC'_sP_{AF}$–$Col_{ob}$–$SmC_sP_{AF}$ reported recently [45]. Nearly all compounds having an odd-numbered spacer prefer the formation of columnar phases and of an undulated SmCP phase. There is one exception: a nematic phase was found for dimer **6-E$_2$** with 11 methylene groups in the spacer.

Concerning the reversion of the carboxylic groups $E_1$ to $E_4$, not all possible combinations have been prepared in the series **1-E** to **7-E**. All four ester groups were changed in their direction – step by step – in the isomeric series **3-E**. On the other hand, the ester linking group $E_2$ was reversed in all series **1-E** to **7-E** which differ in the length of the aliphatic parts (*n, p, m*) to allow a comparison with the corresponding reference compounds **E$_0$**. Referring to Table 1, the mesophase stability of nearly all isomers **E$_1$-E$_4$** is increased after reversing one of the carboxylic groups in the reference compounds **E$_0$**. This allows the preparation of such banana-calamitic twin compounds with thermodynamically stable mesophases. The strongest stabilisation has been observed for the isomers **E$_2$** and amounts up to 32 K (compare **5-E$_0$** with **5-E$_2$**). It is worth mentioning that the directly comparable inversion of the carboxylic group $E_2$ in the corresponding monomeric five-ring bent-core mesogens has a relatively low influence on the mesophase stability, the change of the clearing temperatures for the dodecyloxy substituted compound amounts to −7 K, for the octyloxy homologue +3 K [50]. With growing length of the terminally attached alkyloxy chains there is the tendency in the dimers under study for the clearing temperatures to be reduced. This is in agreement with the mesophase behaviour observed for calamitic systems. For the series with the spacer $m = 6$ (series **2-E** to **5-E**) we could check the influence of the alkyloxy wing groups in more detail. A nearly symmetric substitution ($n = 8$; $p = 6$) yielded the interesting sequence of two nematic phases N–$N_x$ (**2-E$_3$**). For long terminal chains ($n + p >$ 20) the phase behaviour of the non-symmetrically substituted compound **4-E$_2$** ($n = 16$; $p = 6$: N, SmA, $SmC_x$) is very different in comparison to the symmetrically substituted dimer **5-E$_2$** ($n = 12$; $p = 12$: $SmC'_sP_{AF}$ – $SmC_sP_{AF}$).

A further point of interest is the question as to whether the nematic or SmA phases formed by the banana-calamitic dimers under study exhibit the properties of typically calamitic phases, or perhaps more of corresponding phases formed by monomeric bent-core mesogens. In the twin molecules under discussion there is competition between these two moieties. There are clear hints that the physical behaviour of the nematic phases formed by the new dimers **(2–7)-E$_{1–4}$** is comparable in some cases to that reported for corresponding banana-shaped monomers. Chiral domains, as shown in Figure 3, can be observed in the nematic phases of all dimers under study, although the molecules themselves are not chiral. This phenomenon is also observed for nematic phases formed by some monomeric bent-core compounds.

Another subject of interest is the electrically driven pattern formation in nematics, electrohydrodynamic convection. In contrast to conventional calamitic nematics, the nematic phases of the new dimers exhibit a positive dielectric and negative conductivity

anisotropy. Extensive studies have been performed by Stannarius *et al.* using compound **3-E$_2$.** Different pattern types have been described that are distinguished by their respective orientation of the convection roles which can be influenced by frequency, voltage amplitude, and temperature [34, 35, 51]. A further remarkable behaviour of the nematic phase of the banana-calamitic dimer **3-E$_2$** is the field-induced transition from a uniaxial to an optically biaxial nematic state. The biaxially ordered phase persists after the field is removed, but is metastable. The original and the field-induced state can coexist in domains for about 1 h [36]. It goes without saying that such behaviour had been of high interest for the discoverer of the biaxial nematic phase in lyotropic systems, Alfred Saupe [52].

The SmA phases also exhibit unusual properties. This is proved by the experimental finding that the transition temperature SmCP–SmA can be increased on applying an electric field. For compound **4-E$_2$,** this increase amounts to 4 K using 40 V $\mu m^{-1}$. This is clearly more than reported for a comparable monomeric bent-core compound, for which an enhancement of 2 K using 35 V $\mu m^{-1}$ was observed [45].

Summarising the results we can conclude that many new or changed phase sequences have been found by the reversal of ester linking groups of the reference compounds **E$_0$**. Up to now, it has not been possible to predict which phases in which sequences will result from these structural variations, and much more experimental work in this field is needed. Additional work would also be justified in the expectation of new materials with exciting properties.



## Acknowledgement

The Deutsche Forschungsgemeinschaft is acknowledged for financial support.

## References

[1] Vorländer, D. *Z. Phys. Chem*. **1927**, *126*, 449–472.
[2] Imrie, C.T.; Henderson, P.A.; Yeap, G.-Y *Liq. Cryst*. **2009**, *36*, 755–777.
[3] Imrie, C.T.; Henderson, P.A. *Chem. Soc. Rev*. **2007**, *36*, 2096–2124.
[4] Imrie, C.T.; Henderson, P.A. *Curr. Opin. Colloid Interface Sci*. **2002**, *7*, 298–311.
[5] Imrie, C.T. *Struct. Bond.* **1999**, *95*, 149–192.
[6] Imrie C.T.; Luckhurst, G.R. In *Handbook of Liquid Crystals*: Demus, D., Goodby, J.W., Gray, G.W., Spiess, H.W., Vill, V., Eds.; Wiley-VCH: Weinheim, 1998; pp 801–833.
[7] Weissflog, W.; Demus, D.; Diele, S.; Nitschke, P.; Wedler, W. *Liq. Cryst*. **1989**, *5*, 111–122.
[8] Andersch, J.; Tschierske, C.; Diele, S.; Lose, D. *J. Mater. Chem*. **1996**, *6*, 1297–1307.
[9] Andersch, J.; Tschierske, C. *Liq. Cryst*. **1996**, *21*, 51–63.
[10] Surendranath, V.; Lokanath, N.K.; Sridhar, M.A.; Prasad, S.K. *Liq. Cryst*. **1998**, *24*, 361–369.
[11] Weissflog, W.; Lischka, Ch.; Diele, S.; Wirth, I.; Pelzl, G. *Liq. Cryst*. **2000**, *27*, 43–50.
[12] Weissflog, W.; Richter, S.; Dietzmann, E.; Risse, J.; Diele, S.; Schiller, P.; Pelzl, G. *Cryst. Res. Technol*. **1997**, *32*, 271–277.
[13] Niori, T.; Sekine, T.; Watanabe, J.; Furukawa, T.; Takezoe, H. *J. Mater. Chem.* **1996**, *6*, 1231–1233.
[14] Izumi, T.; Kang, S.; Niori, T.; Takanishi, Y.; Takezoe, H.; Watanabe, J. *Jpn. J. Appl. Phys*. **2006**, *45*, 1506–1514.
[15] Takanishi, Y.; Toshimitsu, M.; Nakata, M.; Takada, N.; Izumi, T.; Ishikawa, K.; Takezoe, H.; Watanabe, J.; Takahashi, Y.; Iida, A. *Phys. Rev. E: Stat., Nonlinear, Soft Matter Phys.* **2006**, *74*, 051703-(1-10).
[16] Bialecka-Florjanczyk, E.; Sledzinska, I.; Gorecka, E.; Przedmojski, J. *Liq. Cryst*. **2008**, *35*, 401–405.
[17] Lagerwall, J.P.F.; Giesselmann, F.; Wand, M.D.; Walba, D.M. *Chem. Mater*. **2004**, *16*, 3606–3615.
[18] Eremin, A.; Diele, S.; Pelzl, G.; Kovalenko, L.; Pelz, K.; Weissflog, W. *Liq. Cryst*. **2001**, *28*, 1451–1461.
[19] Pelzl, G.; Diele, S.; Weissflog, W. *Adv. Mater*. **1999**, *11*, 707–724.
[20] Amaranatha Reddy, R.; Tschierske, C.; *J. Mater. Chem*. **2006**, *16*, 907–961.
[21] Takezoe, H.; Takanishi, Y. *Jap. J. Appl. Phys*. **2006**, *45*, 597–625.
[22] Dantlgraber, G.; Diele, S.; Tschierske, C. *Chem. Commun*. **2002**, 2768–2769.
[23] Achten, R.; Koudijs, A.; Giesberg, M.; Marcelis, A.T.M.; Sudhölter, E.J.R.; Schröder, M.W.; Weissflog, W. *Liq. Cryst*. **2007**, *34*, 59–64.
[24] Keith, C.; Amaranatha Reddy, R.; Baumeister, U.; Hahn, H.; Lang, H.; Tschierske, C. *J. Mater. Chem*. **2006**, *16*, 3444–3447.
[25] Keith, C.; Dantlgraber, G.; Amaranatha Reddy, R.; Baumeister, U.; Prehm, M.; Hahn, H.; Lang, H.; Tschierske, C. *J. Mater. Chem*. **2007**, *17*, 3796–3805.
[26] Kosata, B.; Tamba, M.G.; Baumeister, U.; Pelz, K.; Diele, S.; Pelzl, G.; Galli, G.; Samaritani, S.; Agina, E.V.; Boiko, N.I.; Shibaev, V.P.; Weissflog, W. *Chem. Mater*. **2006**, *18*, 691–701.
[27] Umadevi, S.; Sadashiva, B.K.; Shreenivasa Murthy, H.N.; Raghunathan, V.A. *Soft Matter* **2006**, *2*, 210.
[28] Umadevi, S.; Sadashiva, B.K. *Liq. Cryst*. **2007**, *34*, 673–681.
[29] Yelamaggad, C.V.; Prasad, S.K.; Nair, G.G.; Shashikala, I.S.; Rao, D.S.S.; Lobo, C.V.; Chandrasekhar, S. *Angew. Chem. Int. Ed*. **2004**, *43*, 3429–3432.
[30] Prasad, S.K.; Nair, G.G.; Rao, D.S.S.; Lobo, C.V.; Shashikala, I.S.; Yelamaggad, C.V. *Mol. Cryst. Liq. Cryst*. **2005**, *437*, 211–221.
[31] Yelamaggad, C.V.; Nagamani, S.A.; Hiremath, S.A.; Nair, G.G. *Liq. Cryst*. **2001**, *28*, 1009–1015.
[32] Jakli, A.; Liao, G.; Shashikala, I.; Hiremath, U.S.; Yelamaggad, C.V. *Phys. Rev. E: Stat., Nonlinear, Soft Matter Phys.* **2006**, *74*, 041706-(1-6).
[33] Tamba, M.G.; Kosata, B.; Pelz, K.; Diele, S.; Pelzl, G.; Vakhovskaya, Z.; Kresse, H.; Weissflog, W. *Soft Matter* **2006**, *2*, 60–65.
[34] Heuer, J.; Stannarius, R.; Tamba, M.-G.; Weissflog, W. *Phys. Rev. E: Stat., Nonlinear, Soft Matter Phys.* **2008**, *77*, 056206-(1-11).
[35] Stannarius, R.; Heuer, J. *Eur. Phys. J. E: Soft Matter Biol. Phys.* **2007**, *24*, 27–33.

[36] Stannarius, R.; Eremin, A.; Tamba, M.-G.; Pelzl, G.; Weissflog, W. *Phys. Rev. E: Stat., Nonlinear, Soft Matter Phys.* **2007**, *76*, 061704-(1-7).
[37] Miyasato, K.; Abe, S.; Takezoe, H.; Fukuda, A.; Kuze, E.; *Jpn. J. Appl. Phys*. **1983**, *22*, L661–L663.
[38] Tamba, M.-G.; Baumeister, U.; Pelzl, G.; Weissflog, W., to be submitted for publication.
[39] Pelzl, G.; Eremin, A.; Diele, S.; Kresse, H.; Weissflog, W. *J. Mater. Chem*. **2002**, *12*, 2591–2593.
[40] Weissflog, W.; Sokolowski, S.; Dehne, H.; Das, B.; Grande, S.; Schröder, M.W.; Eremin, A.; Diele, S.; Pelzl, G.; Kresse, H. *Liq. Cryst*. **2004**, *31*, 923–933.
[41] Kovalenko, L.; Schröder, M.W.; Amaranatha Reddy, R.; Diele, S.; Pelzl, G.; Weissflog, W. *Liq. Cryst*. **2005**, *32*, 857–865.
[42] Schröder, M.W.; Diele, S.; Pelzl, G.; Dunemann, U.; Kresse, H.; Weissflog, W. *J. Mater. Chem*. **2003**, *13*, 1877–1882.
[43] Weissflog, W.; Schröder, M.W.; Diele, S.; Pelzl, G. *Adv. Mater*. **2003**, *15*, 630–633.
[44] Schroeder, M.W.; Pelzl, G.; Dunemann, U.; Weissflog, W. *Liq. Cryst*. **2004**, *31*, 633–637.
[45] Shreenivasa Murthy, H.N.; Bodyagin, M.; Diele, S.; Baumeister, U.; Pelzl, G.; Weissflog, W. *J. Mater. Chem*. **2006**, *16*, 1634–1643.
[46] Weissflog, W.; Shreenivasa Murthy, H.N.; Diele, S.; Pelzl, G. *Phil. Trans. R. Soc. A (London)* **2006**, *364*, 2657–2679.
[47] Pelzl, G.; Weissflog, W. In *Thermotropic Liquid Crystals – Recent Advances*: Ramamoorthy, A., Ed.; Springer: Dordrecht, the Netherlands, 2007; pp 1–54.
[48] Pelzl, G.; Diele, S.; Jakli, A.; Weissflog, W. *Liq. Cryst*. **2006**, *33*, 1513–1518.
[49] Coleman, D.A.; Fernsler, J.; Chattham, N.; Nakata, M.; Takanishi, Y.; Korblova, E.; Link, D.R.; Shao, R.-F.; Jang, W.G.; Maclennan, J.E.; Mondainn-Monval, O.; Boyer, C.; Weissflog, W.; Pelzl, G.; Chien, L.-C.; Zasadzinski, J.; Watanabe, J.; Walba, D.M.; Takezoe, H.; Clark, N.A. *Science* **2003**, *301*, 1204–1211.
[50] Weissflog, W.; Naumann, G.; Kosata, B.; Schroeder, M.W.; Eremin, A.; Diele, S.; Kresse, H.; Friedemann, R.; Ananda Rama Krishnan, S. *J. Mater. Chem*. **2005**, *15*, 4328–4337.
[51] Tamba, M.G.; Weissflog, W.; Eremin, A.; Heuer, J.; Stannarius, R. *Eur. Phys. J. E: Soft Matter Biol. Phys.* **2007**, *22*, 85–95.
[52] Yu, L.J.; Saupe, A. *Phys. Rev. Lett*. **1980**, *45*, 1000–1003.